AD-A173 143 DIRECT NUMERICAL SIMULATION OF AN UNPREMIXED JET FLAME 1/1
(U) FLOW RESEARCH CO KENT WA P GIVI ET AL. MAR 86
FLOW-TR-369 AFOSR-TR-86-1063 F49620-85-C-0067

UNCLASSIFIED F/G 21/2 NL

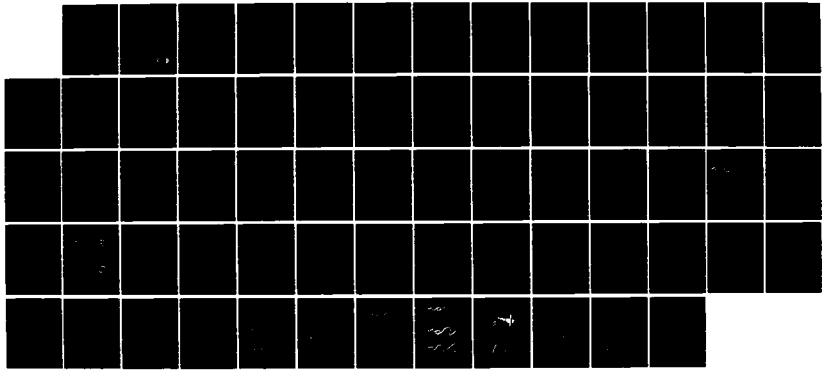

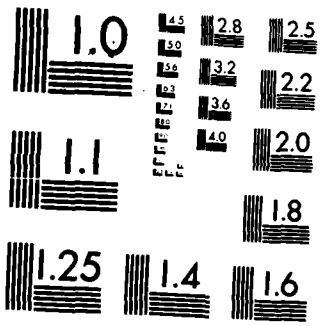

MICROCOPY RESOLUTION TEST CHART
NATIONAL BUREAU OF STANDARDS-1963-A

Flow Technical Report No. 369

DIRECT NUMERICAL SIMULATION OF AN UNPREMIXED JET FLAME

AFOSR-TR- 86-1063

Annual Report
(February 16, 1985 - February 16, 1986)

by
P. Givi, W.-H. Jou and
R. W. Metcalfe

Approved for public release;
distribution unlimited.

March 1986

Flow Research Company
21414-68th Avenue South
Kent, Washington 98032
(206) 872-8500

REPORT DOCUMENTATION PAGE

1a. REPORT SECURITY CLASSIFICATION Unclassified	1b. RESTRICTIVE MARKINGS None
2a. SECURITY CLASSIFICATION AUTHORITY	3. DISTRIBUTION/AVAILABILITY OF REPORT Approved for public release, distribution unlimited
2b. DECLASSIFICATION/DOWNGRADING SCHEDULE	
4. PERFORMING ORGANIZATION REPORT NUMBER(S) Flow Technical Report No. 369	5. MONITORING ORGANIZATION REPORT NUMBER(S) AFOSR-TR- 86-1063
6a. NAME OF PERFORMING ORGANIZATION Flow Industries, Inc.	6b. OFFICE SYMBOL (If applicable)
7a. NAME OF MONITORING ORGANIZATION Air Force Office of Scientific Research	
6c. ADDRESS (City, State and ZIP Code) 21414-68th Avenue South Kent, Washington 98032	7b. ADDRESS (City, State and ZIP Code) Bolling AFB, D.C. 20332-6448
8a. NAME OF FUNDING/SPONSORING ORGANIZATION Air Force Office of Scientific Research	8b. OFFICE SYMBOL (If applicable) AFOSR/NA
9. PROCUREMENT INSTRUMENT IDENTIFICATION NUMBER F49620-85-C-0067	
8c. ADDRESS (City, State and ZIP Code) Bolling AFB, D.C. 20332-6448	10. SOURCE OF FUNDING NOS. PROGRAM ELEMENT NO.: 61102F; PROJECT NO.: 2308; TASK NO.: A2; WORK UNIT NO.:
11. TITLE (Include Security Classification) Direct Numerical Simulation of an Unpremixed Jet Flame	
12. PERSONAL AUTHOR(S) P. Givi, W.-H. Jou, and R. W. Metcalfe	
13a. TYPE OF REPORT Annual	13b. TIME COVERED FROM 2/85 TO 2/86
14. DATE OF REPORT (Yr., Mo., Day) March 1986	15. PAGE COUNT 61
16. SUPPLEMENTARY NOTATION	

17. COSATI CODES		
FIELD	GROUP	SUB. GR.
21	01	
21	02	

18. SUBJECT TERMS (Continue on reverse if necessary and identify by block number)

19. ABSTRACT (Continue on reverse if necessary and identify by block number)

Direct numerical simulations have been employed to study the effects of large coherent structures in two-dimensional, unpremixed, chemically reacting mixing layers under both temporally evolving and spatially developing assumptions. In the temporally evolving mixing layer calculations, a temperature-dependent chemical reaction was incorporated into a computer code that uses pseudospectral numerical methods. The nonequilibrium effects leading to the local quenching of a diffusion flame were investigated. The results indicate that the primary important parameter to be considered for flame extinction is the local instantaneous scalar dissipation rate conditioned at the scalar stoichiometric value. At locations where this value is increased beyond a critical value, the local temperature decreases and the instantaneous reaction rate drops to zero, leading to local quenching of the flame. For the purpose

20. DISTRIBUTION/AVAILABILITY OF ABSTRACT UNCLASSIFIED/UNLIMITED ☒ SAME AS RPT. ☐ DTIC USERS ☐	21. ABSTRACT SECURITY CLASSIFICATION Unclassified
22a. NAME OF RESPONSIBLE INDIVIDUAL Julian M. Tishkoff	22b TELEPHONE NUMBER (Include Area Code) (202)767-4935
22c. OFFICE SYMBOL AFOSR/NA	

Block #19 (cont.)

of simulating spatially developing flows, a two-dimensional, hybrid pseudo-spectral-finite difference code was constructed. The resulting code was tested with simulations of the pretransitional region of laboratory mixing layers. Examination of some of the statistical quantities obtained from the results of these simulations are in qualitative agreement with recent experimental data obtained at the California Institute of Technology and Stanford University. The asymmetric nature of the mixing processes has been numerically simulated.

TABLE OF CONTENTS

OBJECTIVES

The objectives of this work are to develop and implement numerical techniques that will enable us to perform simulations of spatially evolving phenomena. In particular, we are interested in studying the phenomenon of turbulent diffusion flame lift-off.

The flame lift-off phenomenon occurs when the speed of the fuel jet exceeds a certain value. The flame detaches from the exit and is stabilized at a certain distance downstream. Different mechanisms have been proposed to explain the lift-off phenomenon. Generally, it is believed that the phenomenon is similar to that in premixed gas combustion (Brzustowski, 1980; Gunther et al., 1981). At the jet exit, the velocity of the fluid in the mixing layer is higher than the flame propagation speed. The flame cannot be stabilized at that location. As the mixing proceeds, the velocity of the fluid in the mixing layer, where the species ratio roughly becomes stoichiometric, decreases to the flame speed. The flame is stabilized at that position. This model assumes that the mixing of the fuel and the oxidizer as predicted by the nonreacting turbulence model reaches the molecular level everywhere in the mixing layer. Direct numerical simulations of a reacting mixing layer (Riley et al., 1986) indicated that this may not be the case.

Another model was suggested by Peters and Williams (1983). They proposed that, in a turbulent mixing layer, the turbulent eddies produce highly stretched and contorted sheets across which molecular diffusion of species occurs. Combustion appears as laminar flamelets on these sheets. Based on the theory that a laminar flame will extinguish itself if the strain rate is sufficiently high that the local reduced Damkohler number is lower than a critical value (Linan, 1974), Peters and Williams predicted that the strain rate near the exit of the jet is too high for the flame to exist. As the mixing layer grows, the strain rate is reduced to a sufficiently low level that a flame can be sustained. They proceeded to estimate the strain rate in the mixing layer. Through a statistical theory that predicts disruption of a continuous sheet due to "holes" on the sheet, they were able to obtain quantitative results for lift-off distance. Their theoretical predictions of lift-off heights are of the right "order of magnitude" for limited methane flame data.

The results of Peters and Williams, based on simple turbulence models, are encouraging. However, a detailed numerical simulation of the interaction between fluid dynamical and combustion processes that occur in diffusion flames would be invaluable to further our understanding of the physics.

Direct numerical simulations consist of accurately solving appropriate convection-diffusion-reaction transport equations by means of very accurate numerical algorithms so that no turbulence modeling is required. The direct numerical simulation technique has recently been successfully applied to chemically reacting flows. Riley et al. (1986) considered the three-dimensional temporally growing mixing layer under the simplest possible assumption of a constant-rate chemical reaction with no heat release. The main contribution of this work is the understanding of the effects of three-dimensional mixing and diffusion of the species on the chemical reaction. McMurtry et al. (1985) considered the effects of chemical heat release and the resulting density variation on the fluid motion for a two-dimensional mixing layer. The fluid dynamics and the chemical reaction are truly coupled in this work, and the interplay between the two are discussed. However, the assumption of a constant chemical reaction is still employed. We intend to extend the simulations to study the local quenching and the lift-off of a diffusion flame.

The existing methods must be modified to include (1) a temperature-dependent chemical reaction rate and (2) a spatially developing flow. The objective of our first year's work is to examine these features in a two-dimensional mixing layer simulation. The results of the present work can then be extended to three-dimensional simulations in subsequent years.

STATUS OF THE RESEARCH

Our efforts in the past year were concentrated in two main areas: (1) the incorporation of a temperature-dependent reaction rate into a previously developed computer code and the eduction of relevant physics related to flame extinction from the simulation and (2) the development of new numerical algorithms for computing a spatially developing reacting shear layer, which will enable us to address the flame stability and lift-off phenomena in the future. In the first area, temporally evolving mixing layers were considered, while in the second area, spatially developing plane jets and mixing layers

were considered. In both areas, relevant experimental measurements were reviewed and qualitative comparisons with data were made whenever possible. In this section, a brief review of our results and the major conclusions drawn from the research to date in both areas is given. A work plan for the coming year is also presented. Appendices A and B include detailed descriptions of the research.

Summary of Simulations of Temporally Growing Flows

The mechanism of flame extinction was studied through a two-dimensional simulation of a temporally growing mixing layer (Appendix A). A binary, single-step, Arrhenius-type chemical reaction with finite rate chemical kinetics between two unpremixed species was considered. A previously developed two-dimensional numerical code was modified to include the temperature-dependent reaction rate constant. The simulations were performed with a fairly large Zeldovich number (Ze = 20 based on the activation energy and ambient temperature), a moderate Reynolds number (Re = 200 based on the shear layer thickness and the velocity difference across the layer), and a moderate Damkohler number (Da = 10 based on the pre-exponential factor, the velocity difference across the layer and the shear layer thickness). The nonequilibrium phenomenon leading to the local quenching of the diffusion flame was simulated on a 64 X 64 grid computational domain. The results indicate that the large coherent structures have a major influence on the local extinction of the diffusion flame. It was found that the roll up of the unstable shear layer creates regions with high dissipation rates at the braids of the large-scale structure, where local flame extinction occurs. The results indicate that the local mixture temperature drops to a value close to ambient at the braids and the reaction rate reduces to zero, even though the reactants are well mixed there. This is consistent with the theory of Peters and Williams (1983). Within the limitations of our numerical resolution, comparisons of the critical scalar dissipation rate with that obtained by large activation energy asymptotics showed reasonable agreement.

Summary of Simulations of Spatially Developing Flows

In this task, we are mainly interested in the development of numerical codes that are capable of simulating spatially developing flows. In particular, the implementation of the inflow/outflow boundary conditions and

their effect on the interior of the computational domain is addressed. Presently, we have finished constructing a numerical code that is capable of simulating two-dimensional mixing layers and plane jets. For the purpose of demonstration, this code was used for the simulation of the asymmetric mixing in parallel two-stream mixing layers and was used to examine the role of large coherent structures in the enhancement of chemical reactions that occur in such flows (Appendix B).

The flow in the cross-stream direction may be assumed periodic. Therefore, pseudospectral discretization was used in that direction. In the streamwise direction, however, the flow is not periodic. Appropriate inflow/outflow boundary conditions must be applied. At the inflow, a small perturbation, in the form of the most unstable mode and its subharmonics, was added to a mean hyperbolic tangent velocity profile. This pertubation initiated vorticity rollup and pairing of the vortices in the computational domain. The downstream outflow boundary is a computational antifact and is not a natural flow boundary. Therefore, the boundary conditions are difficult to formulate in a rigorous sense. So far, we have employed a zero-gradient condition on the velocity field and the species field and have not tested other possibilities. However, computations were performed with different sizes of the computational domain in the streamwise direction, and the results indicated that this artificial boundary condition at the outflow does not seem to influence significantly the flow field in the interior of the computational domain. To construct the first working code, we employed an overall second-order finite-difference scheme. The convective term is discretized by a quadratic upwind difference scheme in which the leading dispersive truncation error of the second-order central scheme is removed. This results in an improvement of the capability in resolving sharp gradients in a moderate Reynolds number flow over the second-order central scheme. It also improves the stability property over the latter. Second-order central differencing requires a maximum cell Reynolds (Peclet) number of 2, which requires an excessive and nonpractical number of grid points in the streamwise direction. With the upwinding scheme, we were able to simulate a two-dimensional flow with Reynolds and Peclet numbers of about 50 in a domain with 128 X 64 grid points successfully and with no numerical oscillations. Employing a spectral element method (presently under construction) in the streamwise direction should allow us to simulate flows with higher Reynolds numbers.

The resulting code was used to study the effects of large-scale vortex dynamics on a spatially developing, reacting mixing layer. A fast chemistry model, based on the solution of a conserved Shvab-Zeldovich scalar variable, was used to describe the effects of the chemical reactions. Note that making such an assumption about the chemical reactions will not allow us to investigate the the nonequilibrium effects leading to the local quenching of the diffusion flame. However, within this assumption, important information on the convolution of the flame can still be obtained. The results of the numerical simulations indicate that the large coherent structures have a major influence in stretching the stream surface area on which chemical reactions occur, thereby increasing the total amount of product formed in the reaction zone. Furthermore, the results exhibit the experimentally observed asymmetric properties of the entrainment mechanism in the core of the layer (Appendix B).

Current Activities

We are currently incorporating the temperature-dependent reaction rate into the code for spatially developing flow. The resulting code should enable us to simulate the local quenching phenomena in such a flow. We are also developing a three-dimensional code with the option of using either a finite-difference or a spectral element method in the streamwise direction. The resulting code can be use to study three-dimensional turbulent fields in a spatially evolving mixing layer and the structure of "holes" on the flame sheet. Variable density effects caused by the heat release will then be added to the code at a later stage.

PUBLICATIONS

The following written manuscripts have resulted from our efforts in the first year:

1. Givi, P., Jou, W.-H., and Metcalfe, R. W., "Flame Extinction in a Temporally Developing Mixing Layer," Manuscript submitted for Presentation at the Twenty-First International Symposium on Combustion, Munich, West Germany, August 1986 (Appendix A).

2. Givi, P., and Jou, W.-H., "Mixing and Chemical Reactions in a Spatially Developing Mixing Layer," Manuscript accepted for presentation at the Spring Technical Meeting of the Combustion Institute, Central States Section, Cleveland, Ohio, May 5-6, 1986 (Appendix B).

INTERACTIONS

In addition to the above-mentioned written manuscripts, parts of our efforts were presented (or are scheduled to be presented) at the following seminars for which no written manuscripts were required:

1. Givi, P., "Direct Numerical Simulation of an Unpremixed Jet Flame," AFOSR/ONR Contractors Meeting on Turbulent Combustion, California Institute of Technology, Pasadena, July 23-25, 1985.

2. Jou, W.-H., "Numerical Simulation of Chemically Reacting Flows," Invited Presentation, JANAF Workshop on "Coherent Structures in Turbulent Flows", October 1985.

3. Givi, P., "Direct Numerical Simulations of a Reacting Mixing Layer: Bringing Fluid Mechanics Back to Turbulence Research," Invited Seminar, Spring Seminar Series, Department of Mechanical and Aerospace Engineering, State University of New York, Buffalo, March 20, 1986.

REFERENCES

Brzustowski, T. A. (1980) "Mixing and Chemical Reaction in Industrial Flares and Their Models," Physico-Chemical Hydrodynamics, Vol. 1.

Gunther, R., Horch, K., and Lenze, B. (1981) "The Stabilization Mechanism of Free Jet Diffusion Flames," First Specialists Meeting (International) of The Combustion Institute, The Combustion Institute, Pittsburgh, pp. 117-122.

Linan, A. (1974) Acta Astronautica, Vol. 1, p. 1007.

McMurtry, P. A., Jou, W.-H., Riley, J. J., and Metcalfe, R. W. (1985) AIAA paper 85-0143. Also to appear in AIAA Journal.

Peters, N., and Williams, F. A. (1983) AIAA Journal, Vol. 21, pp. 423-429.

Riley, J. J., Metcalfe, R. W., and Orszag, S. A. (1986) Physics of Fluids, Vol. 29, No. 2, pp. 406-422.

APPENDIX A

Flame Extinction in a Temporally Developing Mixing Layer

FLAME EXTINCTION IN A TEMPORALLY DEVELOPING MIXING LAYER

by

P. GIVI, W.-H. JOU and R. W. METCALFE

Flow Research Company

21414-68th Avenue South

Kent, Washington 98032

December 1985

Manuscript Submitted for Presentation at the

TWENTY-FIRST INTERNATIONAL SYMPOSIUM ON COMBUSTION

Subject Matter

10, 11

FLAME EXTINCTION IN A TEMPORALLY DEVELOPING MIXING LAYER

P. GIVI, W.-H. JOU and R. W. METCALFE

Abstract

Nonequilibrium effects leading to the local quenching of a diffusion flame have been investigated by examining the evolution of large-scale structures in a two-dimensional temporally developing mixing layer. Pseudospectral calculations of a temperature-dependent, nonpremixed, reacting shear layer indicate that the primary important parameter to be considered for the flame extinction is the local instantaneous scalar dissipation rate, conditioned at the scalar stoichiometric value (X_{st}). At locations where this value is increased beyond a critical value (X_q), the local temperature decreases and the instantaneous reaction rate drops to zero. This is consistent with the results of the perturbation methods employing large activation energy asymptotics for the study of flame extinction in nonpremixed flames.

1. Introduction

A diffusion flame is characterized by a chemical reaction time that is usually much smaller than a characteristic diffusion time. The chemical reactions occur in a narrow zone between the fuel and the oxidizer, where the concentrations of both reactants are very small. The rate at which the reactants flow into the reaction zone, and therefore the characteristic time of the flame, is dependent on the hydrodynamics of the particular flow. As the characteristic time of the chemical reactions decreases, this reaction region becomes infinitesimally thin. In this limit the chemical reaction zone approaches a "flame sheet" (local chemical equilibrium[1]), where the concentrations of both reactants are very low and the rate of combustion is governed by the rate at which fuel and oxidizer flow into the reaction zone. The flame sheet assumption is justified by the very fast chemical reaction rate of the diffusion flame. This assumption significantly reduces the complexity of the problem since it eliminates the analysis associated with the chemical kinetics. For many flows whose characteristic time scale of chemical reaction is much

smaller than the hydrodynamic (convective-diffusive) time scale, the assumption of local chemical equilibrium adequately predicts the location and the shape of the flame.[2] One important feature of the calculations based on the fast chemistry model is the introduction of a passive Shvab-Zeldovich[2] conserved scalar variable (Z), which is independent of the chemical kinetics. From this quantity, the evolution of the concentration fields of both the reactants and the products can be computed.

In turbulent flows, however, the local characteristic flow time scales vary considerably. As a result, many important and interesting problems that cannot be analyzed by local chemical equilibrium assumptions are introduced. Experimental studies of Tsuji[3] show that as the local characteristic diffusion time becomes shorter and approaches the order of magnitude of the chemical time scale, the details of the chemical reactions cannot be neglected. If the flow of reactants into the reaction zone increases further, causing the diffusion time scale to be reduced more, the chemical reaction will not be able to keep pace with the further supply of reactants. The reaction rate will be reduced, and local quenching occurs. As shown by Peters,[4] further reduction of the diffusion time scale leads to lift-off and the blow-off of the entire flame. As noted by both Tsuji and Peters, the consideration of flame extinction cannot be explained by the flame sheet model, which assumes an infinitely fast chemical reaction rate. Therefore, in order to address the quenching phenomenon, the structure of a finite reaction rate zone must be studied.

There are a number of possible ways to account for the influence of finite rate chemistry on a diffusion flame. For laminar flows, a full set of conservation equations with one- or two-step kinetics has been solved by numerical methods.[5] With simplified kinetics, perturbation methods based on

large Damkohler number asymptotics[6,7] or on large activation energy asymptotics[8,9] have proven useful. Damkohler number asymptotics give some estimate of the broadening of the reaction zone in nonequilibrium situations. The analysis of extinction and ignition cannot be addressed by this method, however, but can be analyzed by activation energy asymptotics. (For a detailed summary and review of the different perturbation techniques, see Ref. 2.)

Linan[9] has employed a method of matched asymptotic expansions in the limit of large activation energy in an attempt to describe the interaction between the hydrodynamics and chemical reactions in the reaction zone of a counterflowing laminar diffusion flame. It has been shown that activation energy asymptotics are very useful in predicting flame ignition and extinction characteristics in such flows. This technique was extended to turbulent flows by Peters[4,10] by considering turbulent diffusion flames as an ensemble of laminar diffusion flamelets.[11] By introducing a local coordinate system that moves with the stoichiometric flame sheet, and employing a perturbation of the large activation energy asymptote, Peters[4] was able to recognize that the primary "nonequilibrium" parameter for the analysis of the flame extinction is the dissipation rate of the scalar quantity evaluated at stoichiometric conditions (X_{st}). This quantity is viewed as the inverse of the diffusion time scale. If this parameter is increased beyond a critical limit (X_q), the heat conducted to both sides of the diffusion flamelets cannot be balanced by the heat production due to chemical reaction. At the critical value of the dissipation, the finite rate kinetics balance the diffusion.[3] Some numerical calculations, performed by Liew et al.[12] and compared with experimental data,[13] show also that as the maximum value of the

dissipation (X_{max}) increases, the value of the maximum temperature decreases, the reaction eventually ceases, and the flame is locally quenched.

These results indicate that the dissipation rate of the conserved scalar is a useful characteristic to study in the analysis of nonequilibrium effects leading to flame extinction. In turbulent flows, however, the quantity X_{st} is a strongly fluctuating quantity that has not yet been numerically computed. Instead, statistical approaches have been chosen by Peters and Williams[14] and Janicka and Peters[15] employing different turbulence closures in predicting the lift-off height of a round diffusion jet flame. Results obtained using these methods were compared with experimental data[16] for both methane and natural gas flames and show some correct order-of-magnitude predictions. These results are encouraging; however, with the availablity of larger computers, it is now possible to employ a more accurate treatment of the flame extinction and local flame quenching that occur in nonpremixed flames. It would be very useful to correlate the flame extinction with the nonequilibrium parameter X_{st}. Also, it would be very interesting to look at the structure of the diffusion flames at the point of extinction. These are the objectives of this paper.

The present paper employs a direct numerical simulation approach to investigate the problem of local flame extinction in a time-dependent, two-dimensional mixing layer. In this flow, the governing equations are solved by an accurate numerical method without a closure model. The time-dependent flow field can be analyzed statistically to understand the underlying physics much as an experimentalist does with laboratory data. The direct numerical simulation technique has recently been successfully applied to chemically reacting flows. Riley et al.[17] considered the three-dimensional temporally growing mixing layer under the simplest possible assumption of a constant

rate, non-heat-releasing chemical reaction. The main contribution of the work is the understanding of the effects of three-dimensional mixing and the diffusion of the species on the chemical reactions. McMurtry et al.[18] considered the effects of the chemical heat release and the resulting density variation on the fluid motion for a two-dimensional mixing layer. The fluid dynamics and the chemical reaction are truly coupled in this work, and the interplay between the two are discussed. However, the assumption of a constant chemical reaction rate is still employed. In the present work, we intend to understand the flame extinction problem through a two-dimensional simulation of a mixing layer. In particular, the role of large-scale features of the turbulent flow in flame extinction is studied. Due to limitations of numerical accuracy, only moderate Reynolds and Damkohler numbers are computed. For flame extinction in a three-dimensional turbulent flow, three-dimensional simulations will be performed in the future.

In the following section, the geometrical configuration of the problem is given, together with the formulation of the problem. In Section 3, some sample results are presented. Finally, in Section 4, conclusions are presented.

2. Problem Formulation

For simplicity of numerical calculations, we consider a two-dimensional shear layer as shown in Fig. 1. The reactant C_B flows to the right on the upper stream, and the other reactant, C_A, flows to the left on the lower stream. The flow is considered periodic in the horizontal direction (x). Although the splitter plate flow evolves <u>spatially</u> downstream and the numerical simulations evolve <u>temporally</u>, important similarities in the dynamics of these two flows make it useful to study accurate numerical simulations of the

temporally growing mixing layers. According to the model, a flow quantity averaged in the x-direction can be related to the time average of the same quantity at a fixed location in a splitter plate configuration. These average quantities are dependent on the transverse coordinate (y) and the time (t). Again, the inverse Galilean transformation relates the time t to the streamwise location in a splitter configuration. This allows us to use accurate pseudospectral numerical methods; these methods are discussed in Ref. 17 and will not be repeated here.

Initially, the two chemical species A and B are not premixed. The chemical reaction between the two species is assumed to be single-step and irreversible and to obey the temperature-dependent Arrhenius law. It is assumed that the heat release rate is low so that the effects of the chemical heat release on the flow field can be neglected. This, together with the further assumptions of a low Mach number flow, result in a constant-density flow formulation.

The velocity field ($\underline{U}$) satisfies the incompressible Navier-Stokes equations normalized by the density, which is taken to be unity:

$$\nabla \cdot \underline{U} = 0 \tag{1}$$

$$L(\underline{U}, \nu) = \frac{\partial \underline{U}}{\partial t} + \underline{U} \cdot \nabla \underline{U} - \nu \nabla^2 \underline{U} = - \nabla P \tag{2}$$

The species concentration fields are governed by

$$L(C_A, D) = L(C_B, D) = - W \tag{3}$$

In this equation, the stoichiometric coefficient is set equal to unity, and the reaction rate follows the Arrhenius law:

$$W = A_f \, e^{-E/RT} \, C_A C_B \tag{4}$$

where A_f is the preexponential frequency factor, E is the activation energy, R is the universal gas constant, and T is the temperature, which is governed by its own transport equation.

$$C_v\, L(T, K) = QW \tag{5}$$

To identify the nondimensional groupings, the variables are normalized by a velocity scale (mean velocity difference across the layer ΔU), a temperature scale (free-stream T_∞), concentration scales (free-stream $C_{A\infty}$ and $C_{B\infty}$), and a length scale ($\lambda = 2.249\ \sigma$, where σ is the distance from the plane of symmetry to the transverse plane, where the mean velocity rises to half of its free-stream value). The value of 2.249 was chosen so that the size of the computational domain would be equal to the wavelength of the most unstable mode and its normalized value would be an integer multiple of 2π.

$$\begin{aligned}
\underline{x}^* &= \frac{\underline{x}}{\lambda} & \nabla^* &= \lambda \nabla \\
\underline{U}^* &= \frac{\underline{U}}{\Delta U} & t^* &= t\,\frac{\Delta U}{\lambda} \\
P^* &= \frac{P}{(\Delta U)^2} & T^* &= \frac{T}{T_\infty} \\
C_A^* &= \frac{C_A}{(C_A)_\infty} & C_B^* &= \frac{C_B}{(C_B)_\infty}
\end{aligned} \tag{6}$$

Assuming equal free-stream concentrations, i.e., $C_{A\infty} = C_{B\infty}$, the nondimensionalized equations become

$$\begin{aligned}
&\nabla \cdot \underline{U}^* = 0 \\
&L^*(\underline{U}^*, \mathrm{Re}) = \frac{\partial \underline{U}^*}{\partial t} + \underline{U}^* \cdot \nabla \underline{U}^* - \frac{1}{\mathrm{Re}}\,\nabla^{*2}\,\underline{U}^* = -\nabla P^* \\
&L^*(C_A^*, \mathrm{Re\ Sc}) = L^*(C_B^*, \mathrm{Re\ Sc}) = -W^* \\
&L^*(C_P^*, \mathrm{Re\ Sc}) = W^* \\
&L^*(T^*, \mathrm{Re\ Pr}) = \mathrm{Ce}\ W^*
\end{aligned} \tag{7}$$

where

$$W^* = Da\ e^{-Ze/T^*} C_A^* C_B^*$$

$$Da = \frac{A_f C_\infty}{\frac{\Delta U}{\lambda}} = \text{Damkohler number}$$

$$Ze = \frac{E}{RT_o} = \text{Zeldovich number}$$

$$Re = \frac{\Delta U \lambda}{\nu} = \text{Reynolds number} \qquad (8)$$

$$Ce = \frac{Q}{C_v T_o} = \text{Heat release parameter}$$

$$Sc = \frac{\nu}{D} = \text{Schmidt number}$$

$$Pr = \frac{K}{D} = \text{Prandtl number}$$

Normalization of the equations yields the important nondimensional groupings that appear in the formulation: the Reynolds number, the Damkohler number, the Zeldovich number, the heat release parameter, the Schmidt number, and the Prandtl number. The values of Sc and Pr can be set equal to unity, since this is approximately correct for gaseous diffusion flames. This results in a Lewis number of unity. The value of other nondimensional parameters is limited by the available resolution of the numerics employed in the computations.

Shvab-Zeldovich Variable

For the two-feed diffusion flame considered here, it is possible to consider only three scalar quantities rather than solving for all four scalar variables. The Shvab-Zeldovich variable (Z) and the product concentrations (G), following Givi et al.,[19] are defined as

$$Z = C_A^* + C_P^*$$
$$G = C_P^* \qquad (9)$$

The transport equations governing Z, G, and T^* follow:

$$L^*(Z) = 0$$

$$L^*(G) = Da\, e^{-Ze/T^*} (1 - Z - G)\, (Z - G) \tag{10}$$

$$L^*(T^*) = Ce\, Da\, e^{-Ze/T^*} (1 - Z - G)\, (Z - G)$$

One could further relate the normalized temperature and product concentrations to the normalized Shvab-Zeldovich variable, eliminating the need for the solution of the equation governing G, if the initial conditions for T^* and G could be related.[1] For the moderate Damkohler numbers employed in these calculations, however, the reaction zone at the interface of the two reactants was numerically ignited by increasing the temperature around the reaction surface, resulting in different initial normalized profiles for the product and temperature. Therefore, for the treatment of the nonpremixed system we plan to investigate, the full solution of hydrodynamic variables (U^*, V^*, P^*), scalar variables (Z, G) and temperature (T^*) is required.

Initial and Boundary Conditions

The initial and boundary conditions for the velocity field are given elsewhere[20] and are only summarized here. In terms of the stream function, the initial condition is given by

$$\psi = \psi_{mean} + \psi_f + \psi_{sh} \tag{11}$$

where ψ_{mean} is the stream function associated with a mean hyperbolic tangent velocity profile, ψ_f is the stream function for the most unstable mode of this mean velocity profile, and ψ_{sh} is the stream function for the first subharmonic of the most unstable mode. The properties of these modes have been evaluated from linear stability theory.[21] The fundamental mode in

this mixing layer produces a single vortex rollup, and when the subharmonic is added in, a second rollup, or pairing, can occur.[20] In the computations reported in this paper, we have employed two initial conditions for the hydrodynamics: (1) the mean flow and the fundamental mode alone (Case I), and (2) the mean flow, the fundamental mode, and the first subharmonic mode added together in phase (Case II). In this manner, the effects that the vortex rollup have on the chemical reaction can be examined.

The initial conditions for the reactant concentration are given by

$$C_A^*(x^*, y^*, 0) = \frac{1}{y_o^*\sqrt{\pi}} \int_{-\infty}^{y_o^*} \exp\left(-\frac{\xi^2}{y_o^2}\right) \, d\xi$$

$$C_B^*(x^*, y^*, 0) = 1 - C_A^* \qquad (12)$$

$$C_P^*(x^*, y^*, 0) = 0$$

Note that there are no initial scalar fluctuations in the scalar profiles. This functional form for the initial concentration of the reactants was chosen to give realistic profiles that would be easily resolvable using sine/cosine Fourier expansions. The profile of the product is initially set to zero.

The temperature at the free streams is equal to T_∞. Near $y = 0$, this value is increased to an ignition temperature to allow the chemical reactions to occur. The initial profile for T^* is given by an exponential function.

$$T^*(x^*, y^*, 0) = 1 + 4 \exp\left(-4 y^{*2}\right) \qquad (13)$$

A periodic boundary condition is employed in the streamwise direction, and a free-slip boundary condition in the cross-stream direction. These boundary conditions are natural when Fourier series expansions are used.

3. Presentation of Results

A pseudospectral numerical code developed by McMurtry et al.[18] was modified for the calculations of the incompressible reacting flow considered here. Computations were performed in a square domain with the size $0 < x < 2\pi\lambda$, $-\pi\lambda < y < \pi\lambda$ for the single vortex rollup and the domain $0 < x < 4\pi\lambda$, $-2\pi\lambda < y < 2\pi\lambda$ for the double rollup computations. The spatial resolution is 64x64 Fourier modes. The values of the Reynolds and Damkohler numbers were set equal to 200 and 10, respectively, so that the simulation would be accurately resolved on the 64x64-point grid employed here. The value of the Zeldovich number based on the free-stream temperature was set equal to 20. The value of the heat release parameter was selected to be small enough so that, when multiplied by the Damkohler number, it would be resolvable by the numerics and so that it would also be reasonable to neglect the effects of heat release on the flow field. However, this value should be large enough to allow the effects of temperature dependence on the chemical reaction term. A value of Ce = 8 is satisfactory, giving a maximum (adiabatic) temperature of $T^*_{adiabatic} = 7$. Because of diffusion, the actual maximum temperature at the reaction surface will be less than the above flame temperature obtained under adiabatic conditions.

The velocity profile for incompressible periodic mixing layers has already been documented[17] and will not be discussed here. Instead, the chemical quantities that are of interest in flame extinction problems will be presented. In this section, the instantaneous profiles of the concentration fields, the temperature field, and the local reaction rates are presented and discussed in detail.

The profiles of the conserved Shvab-Zeldovich scalar variable are chosen for the purpose of flow visualization. In Figs. 2 and 3, we present the time

sequence development of this profile for Cases I and II, respectively. Initially, the perturbation associated with the fundamental mode grows until a time of $t^* = 9$, where the first vortex rollup occurs. This results in a very steep gradient of the Shvab-Zeldovich variable near the braids of the vortex rollup due to the high strain field there. Proceeding further in time results in diffusion of the core of the vortex with no additional rollup. Adding the subharmonic associated with this unstable mode results in a second rollup (Fig. 3) that initiates at a time of about $t^* = 12$ and is completed by $t^* = 24$. As shown in these figures, the effect of the vortex dynamics is to increase the strain rate at the braids of the rollup.

If a fast chemistry model was assumed to describe the chemical reactions, the surface of $Z = Z_{st} = 0.5$ would correspond to the flame location. The vortex dynamics plays an important role in increasing the area of the flame surface (Z_{st} surface) and in increasing the total amount of reaction product compared to the case where there is no rollup and the chemical reaction is only limited to the interdiffusion of the scalars at the reaction surface. In the present calculations, the increase of the equilibrium flame sheet surface due to rollup (Case I, Fig. 2c) is 153 percent in comparison with the unforced case. Merging of the vortices (Case II, Fig. 3c) increases this surface by 300 percent when compared with the unforced case.

The time sequence of the product concentration is also shown on Figs. 4 and 5 for Cases I and II, respectively. The mechanism of vortex rollup is to draw the reactants from the two streams to the reaction surface. The amount of products, along the $Z = Z_{st}$ surface, reaches a maximum at the core of the vortex and a minimum at the braids. The same trends are shown by the temperature profiles (Figs. 6 and 7), where the maximum temperature occurs at the core (the hottest location), where vorticity is also highest, and decreases in

the braids, where the gradients of the scalar are at their higher values. At the time where the computation is stopped, the maximum product concentration has not yet reached its equilibrium value. There still remain reactants, even at the core of the mixing layer, and the flame shortening phenomenon, which is usually caused by the depletion of the reactants, has not been yet observed.

The reason for this behavior of the chemical product and temperature can be explained by the contour plots of the instantaneous reaction rate W, presented in Fig. 8 for Case I. As shown on this figure, the reaction rate initially is very much uniform along the species interdiffusion zone and is maximized at the reaction surface, where the reactants are in contact. At later times, the reaction rate decreases, and at points where the strain rate is sufficiently large, the reaction rate goes to zero and the flame locally quenches. This mechanism of extinction of the diffusion flame is consistent with the experimental observations of Tsuji.[3] In the braids, as the inverse of the diffusion time scale ($1/X_{st}$) decreases (as the result of the vortex rollup), the supply of the reactants is greater than the chemical reaction can keep pace with. Notice from Figs. 2 through 5 that the reactants are well mixed on the braids, but the reaction rates at these places are zero. This nonequilibrium phenomenon can be explained by examining the reaction rate equation [Eq. (4)].

Unlike the temperature-independent reacting mixing layer calculation reported by Givi et al.,[22] the maximum value of the reaction rate does not necessarily correspond to the maximum value of the product of the reactants concentration, since the effects of the temperature variations influence the local conversion rate of the chemistry. If the flame temperature goes below a critical characteristic temperature, the flame becomes very rich with both reactants. However, since the value of the dissipation rate is greater than

the critical value, this premixed region of the reactants cannot be reignited from the high temperature zone of the core. A higher dissipation rate results in a further decrease in temperature until it becomes equal to the background temperature. At this point, the vortex has reached the boundary of the computational domain and, therefore, further computation is not realistic.

As mentioned earlier, Peters[4] developed a theory based on the methodology of Linan[9] to obtain a criterion for the critical value of the dissipation rate for an irreversible one-step chemical reaction. Employing large activation asymptotics, he derived an equation for X_q that depends on the frequency factor of the kinetics term, the activation energy, Z_{st}, and the temperature at the stoichiometric value. A direct quantitative comparison of X_q, obtained in our numerical simulations (X_q is approximated here as the value of the instantaneous dissipation rate evaluated at the stoichiometric surface Z_{st}) with that obtained under the large activation energy asymptotics is not expected to agree exactly for several reasons. First, in asymptotic analysis, the flame thickness is very small and is only broadened near the reaction zone by a small parameter. In the direct numerical simulations reported here, the reactants have a fairly "thick" overlap region in the reaction zone due to the numerical accuracy limitations. Furthermore, the initial conditions for the temperature profile employed here near the reaction zone are not the same as the uniform initial temperature distributions of Peters.[4] The value of the initial temperature is very important in the calculation of the adiabatic flame temperature employed in the asymptotic analysis. This was also discussed by Liew et al.[12] in their numerical prediction of the flame extinction. However, making the assumption that the initial concentration of the reactant and the temperature of the reactants are at some average values in the range between the free stream and the reaction zone, correct order-of-magnitude asymptotic

results are verified by the results of the simulations. The temperature profiles presented in Fig. 6 show that by a time of $t^* = 15$, the value of the temperature at the braids falls to about one-fifth the flame temperature (approximately equal to the free-stream temperature). This corresponds to local quenching. The corresponding computed normalized dissipation rate X^*_{st} ($X^*_{st} = X_{st}\lambda/\Delta U$) at the point of quenching, for the given kinetics data, is about 7 for both Cases I and II. The estimated corresponding value for the dissipation rate, computed with the asymptotic methods described above, is about 8, which is in good agreement with the results of the numerical simulation.

4. Conclusions

A pseudospectral algorithm has been used for the numerical calculations of a chemically reacting, temperature-dependent mixing layer. The nonequilibrium effects leading to the local flame quenching have been simulated in a case with fairly large Zeldovich number and moderate Reynolds and Damkohler numbers. It has been found that the rollup of an unstable shear layer creates regions with high dissipation rates at the braids, where local flame extinction occurs according to the theory of Peters[4,14]. The temperature contour shows that the temperature drops to a value close to ambient at the braids and the reaction rate reduces to zero, even though the reactants are well mixed there. Within the limitations of numerical resolution, comparison of the critical scalar dissipation rate with that obtained by large activation energy asymptotics shows reasonable agreement. We are presently expanding this work to investigate a spatially developing mixing layer and three-dimensional turbulent flows. This should further illuminate the basic mechanisms of such phenomena as the diffusion jet flame lift-off.

Nomenclature

A_f	Preexponential factor
C	Concentration
C_v	Specific heat
Ce	Heat release parameter
D	Molecular diffusivity
Da	Damkohler number
E	Activation energy
G	Normalized product concentration
K	Thermal conductivity
L	Convective-diffusive operator
P	Pressure
Pr	Prandtl number
Q	Heat of reaction
R	Universal gas constant
Re	Reynolds number
Sc	Schmidt number
T	Temperature
t	Time
U	Streamwise velocity component
V	Cross-stream velocity component
W	Reaction rate
X	Dissipation
x	Streamwise coordinate
y	Cross-stream coordinate
Z	Shvab-Zeldovich variable
Ze	Zeldovich number

Greek

λ	Length scale
ν	Molecular viscosity
ψ	Stream function

Superscript

*	Non-dimensionzalized

Subscript

A,B	Reactants
f	Fundamental
P	Product
q	Quenching
sh	Subharmonic
st	Stoichiometric
∞	Free stream

Acknowledgments

The calculations reported here were performed under the support of the Air Force Office of Scientific Research, Contract No. F49620-85-C-00067DEF. The authors have also appreciated the support of NASA Lewis Research Center in providing computer time.

References:

1. Bilger, R. W.: Turbulent Reacting Flows (P. A. Libby and F. A. Williams, Eds.), p. 65, Springer-Verlag, 1980.
2. Williams, F. A.: Combustion Theory, Second edition, The Benjamin/Cummings Publishing Company, Inc., 1985.
3. Tsuji, H.: Prog. Energy Comb. Sci. 8, 93 (1982).
4. Peters, N.: Comb. Sci. Tech. 30, 1 (1983).
5. Liu, T. M. and Libby, P. A.: Comb. Sci. Tech. 2, 131 (1970).
6. Fendell, F. E.: J. Fluid Mech. 21, 281 (1965).
7. Allison, R. A. and Clarke, J. F.: Comb. Sci. Tech. 23, 113 (1980).
8. Buckmaster, J. D. and Ludford, G. S. S.: Theory of Laminar Flames, Cambridge University Press, 1982.
9. Linan, A.: Acta Astronautica 1, 1007 (1974).
10. Peters, N.: Prog. Energy Comb. Sci. 10, 319 (1984).
11. Williams, F. A.: Turbulent Mixing in Non-Reactive and Reactive Flows (S. N. B. Murthy, Ed.), p. 189, Plenum Press, 1975.
12. Liew, S. K., Moss, J. B. and Bray, K. N. C.: Dynamics of Flames and Reactive Systems (J. R. Bowen, N. Manson, A. K. Oppenheime and R. I. Sdoukhin, Eds.), Progress in Astronautics and Aeronautics, Vol. 95, p. 305 (1984).
13. Mitchell, R., Sarofin, A. and Clomburg, L.: Comb. and Flame 37, 337 (1980).
14. Peters, N. and Williams, F. A.: AIAA J. 21, 423 (1983).
15. Janicka, J. and Peters, N.: Nineteenth Symposium (International) on Combustion, p. 367, The Combustion Institute, 1982.
16. Donnerhack, S. and Peters, N.: Comb. Sci. Tech. 41, 101 (1984).

17. Riley, J. J., Metcalfe, R. W. and Orszag, S. A.: Phys. Fluids, to appear (1986).

18. McMurtry, P. A., Jou, W.-H., Riley, J. J. and Metcalfe, R. W., AIAA Paper 85-0143, 1985.

19. Givi, P., Sirignano, W. A. and Pope, S. B.: Comb. Sci. Tech. 37, 59 (1984).

20. Riley, J. J. and Metcalfe, R. W., AIAA Paper 80-0274, 1980.

21. Michalke, A.: J. Fluid Mech. 19, 543 (1964).

22. Givi, P., Ramos, J. I. and Sirignano, W. A.: J. Non-Equilibrium Thermodynamics 10, 75 (1985).

Figure Captions

FIG 1. Problem geometry.

FIG 2. Plots of Shvab-Zeldovich variable contours for a sequence of times (Case I).

FIG 3. Plots of Shvab-Zeldovich variable contours for a sequence of times (Case II).

FIG 4. Plots of normalized product concentration contours for a sequence of times (Case I).

FIG 5. Plots of normalized product concentration contours for a sequence of times (Case II).

FIG 6. Plots of normalized temperature contours for a sequence of times (Case I).

FIG 7. Plots of normalized temperature contours for a sequence of times (Case II).

FIG 8. Plots of normalized reaction rate contours for a sequence of times (Case I).

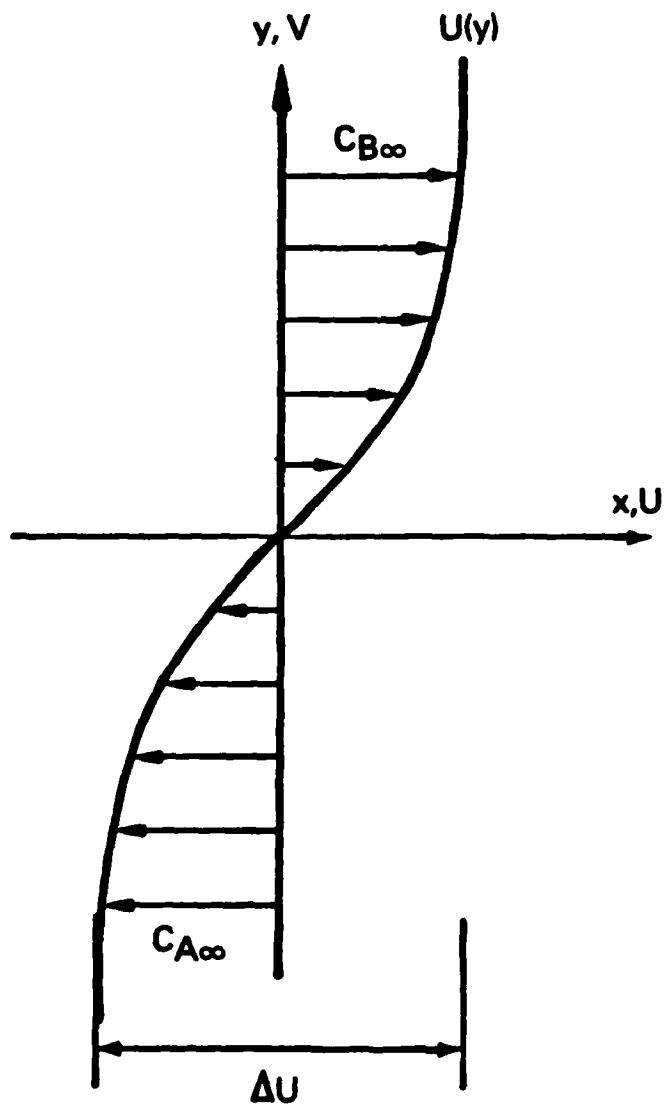

FIG 1. Problem geometry.

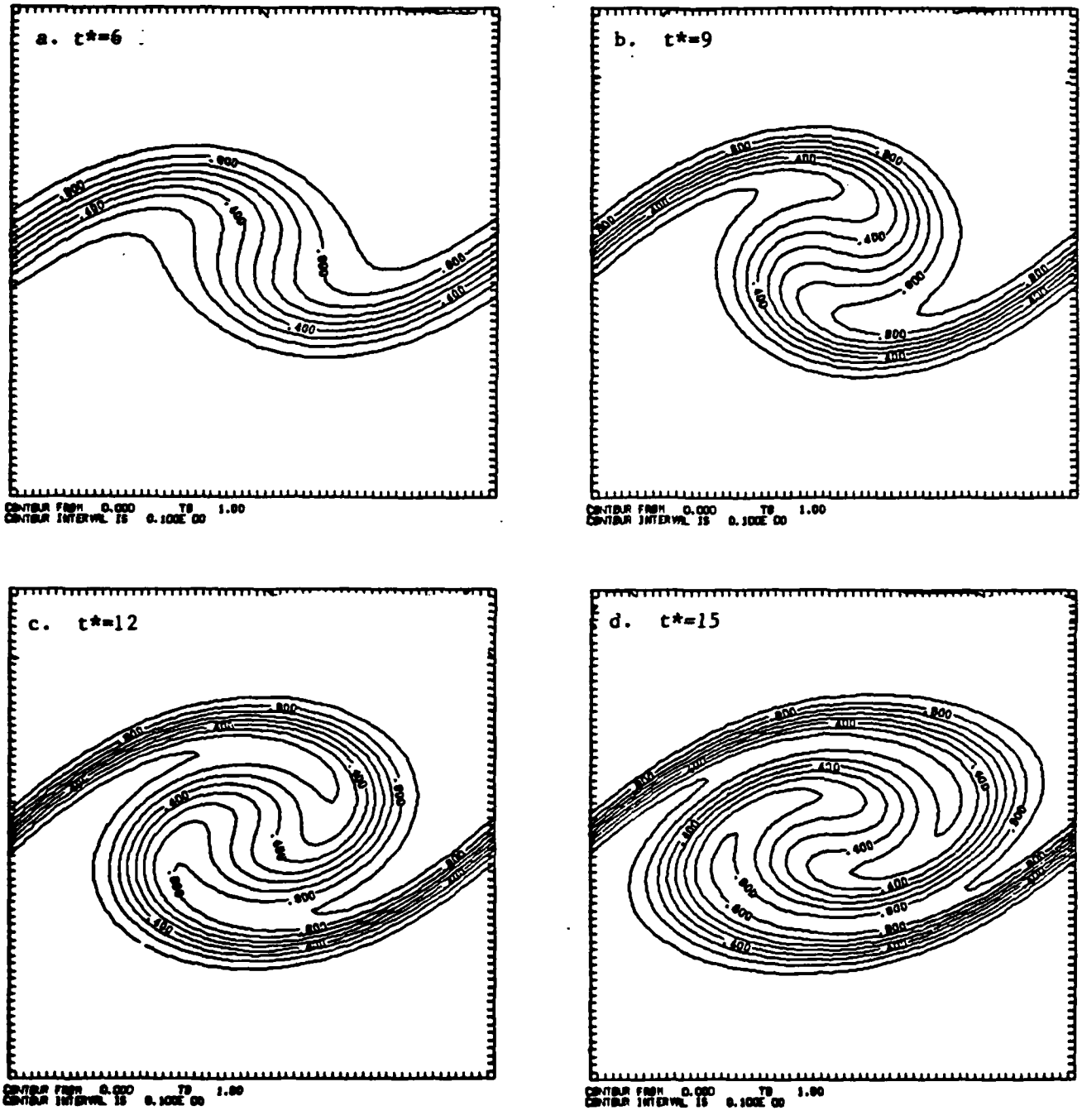

FIG 2. Plots of Shvab-Zeldovich variable contours for a sequence of times (Case I).

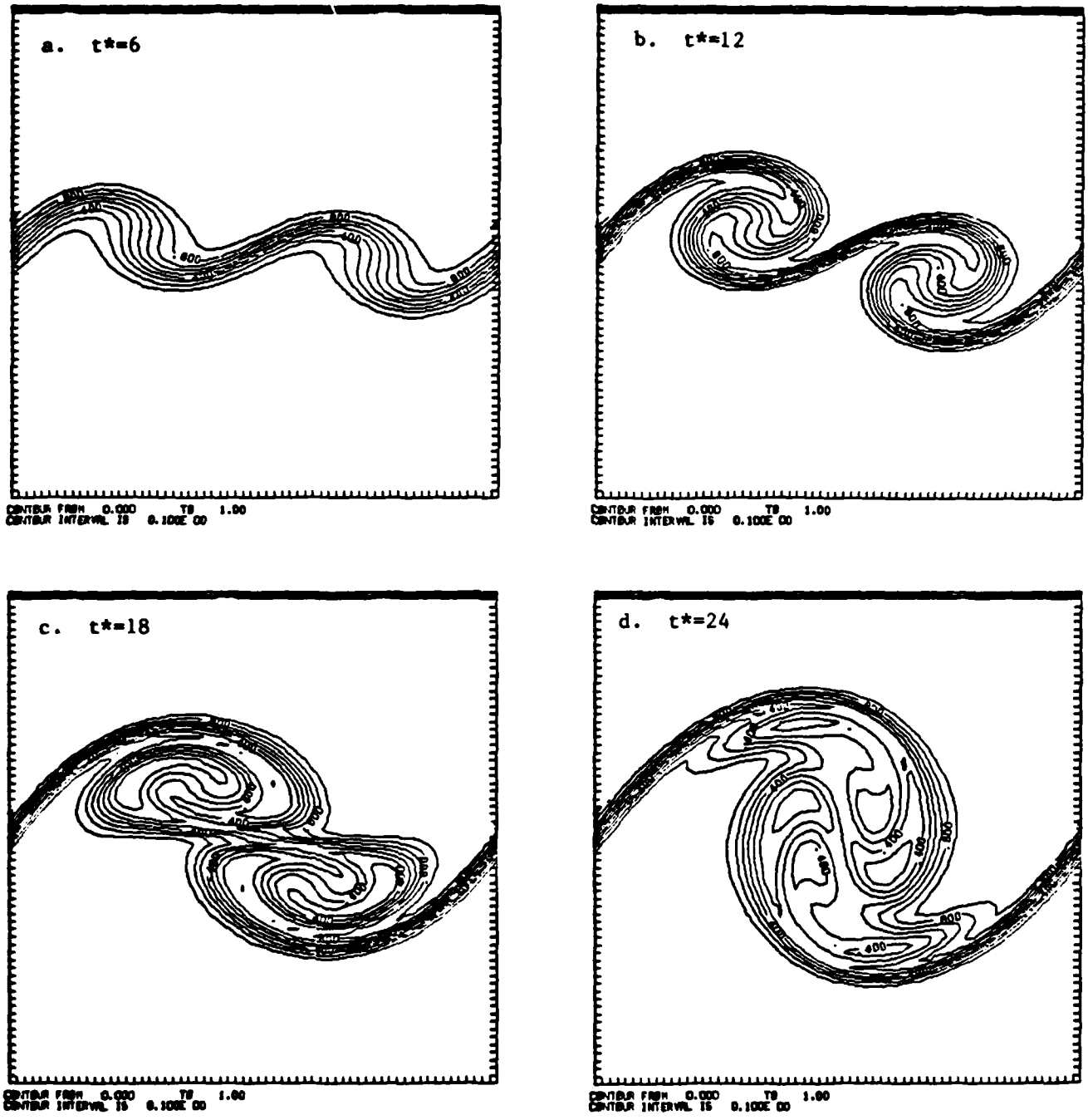

FIG 3. Plots of Shvab-Zeldovich variable contours for a sequence of times (Case II).

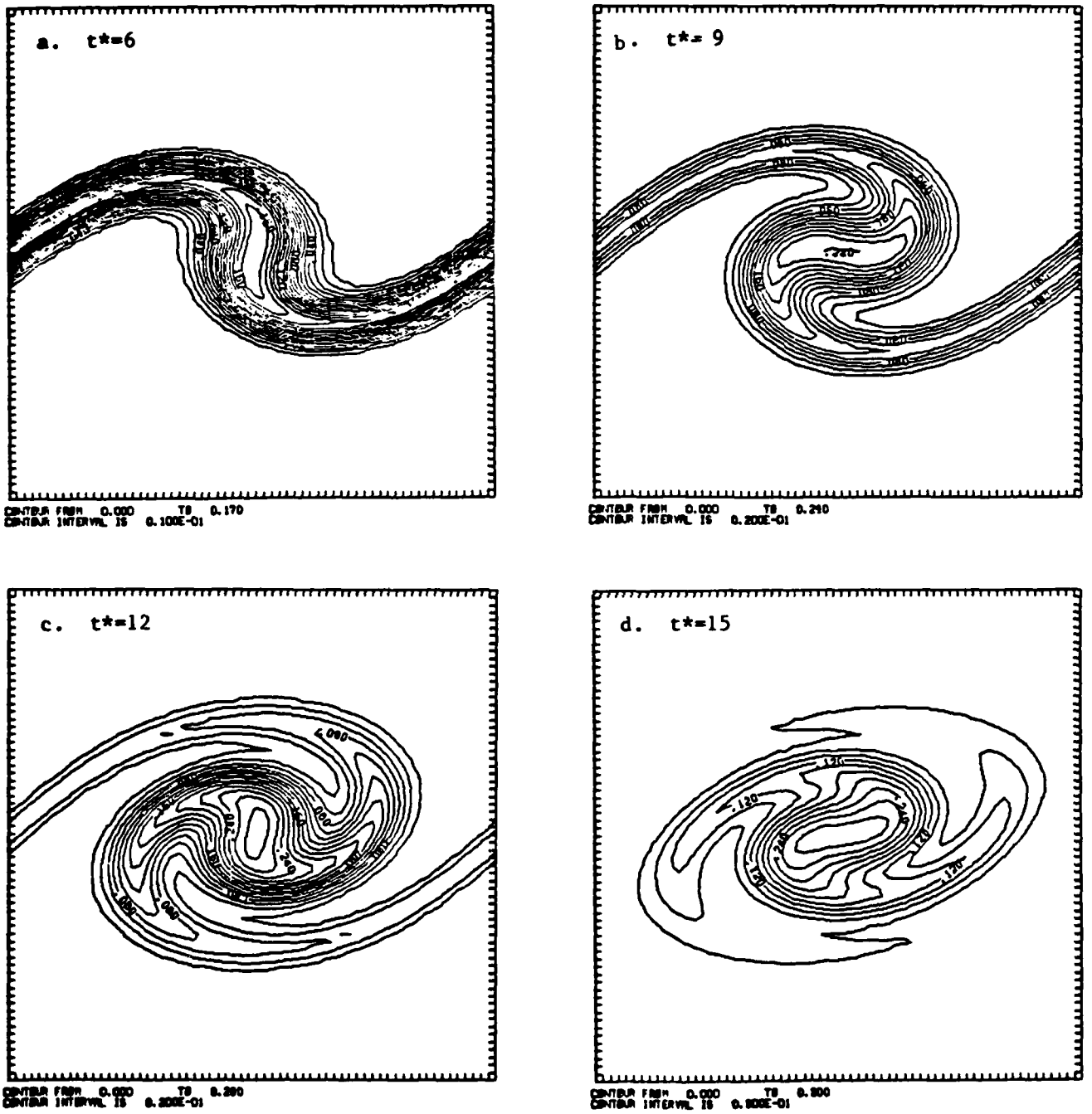

FIG 4. Plots of normalized product concentration contours for a sequence of times (Case I).

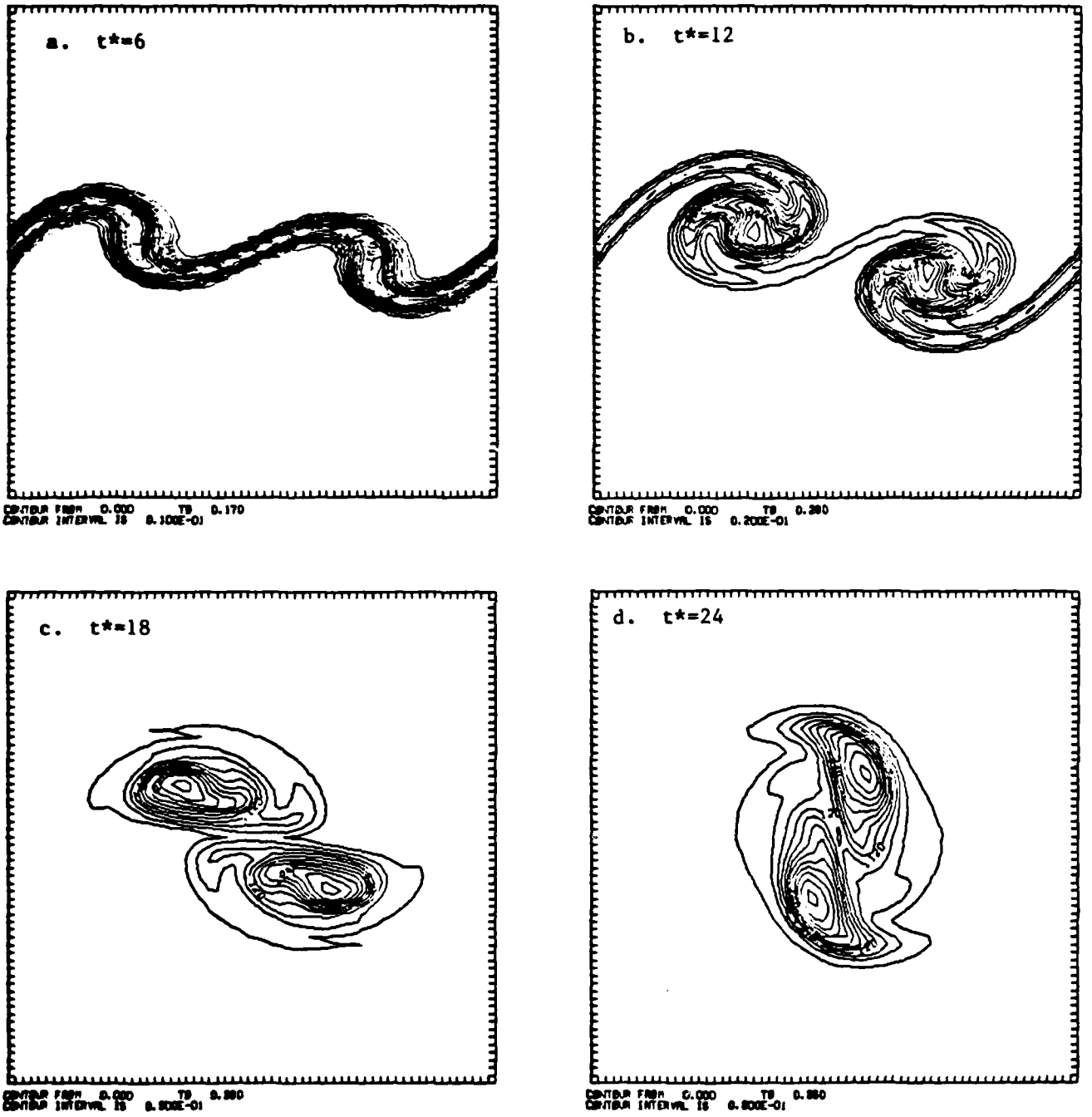

FIG 5. Plots of normalized product concentration contours for a sequence of times (Case II).

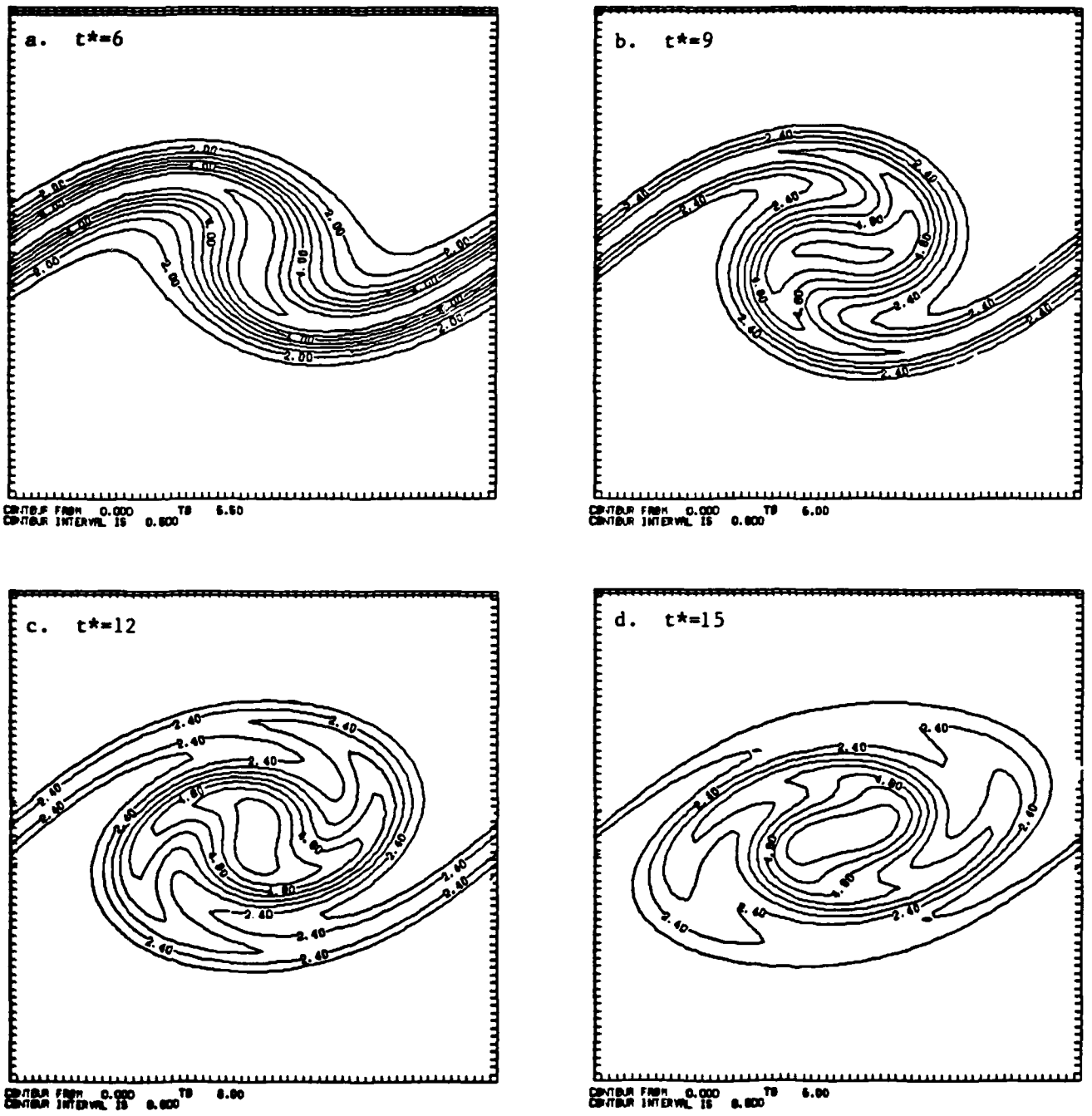

FIG 6. Plots of normalized temperature contours for a sequence of times (Case I).

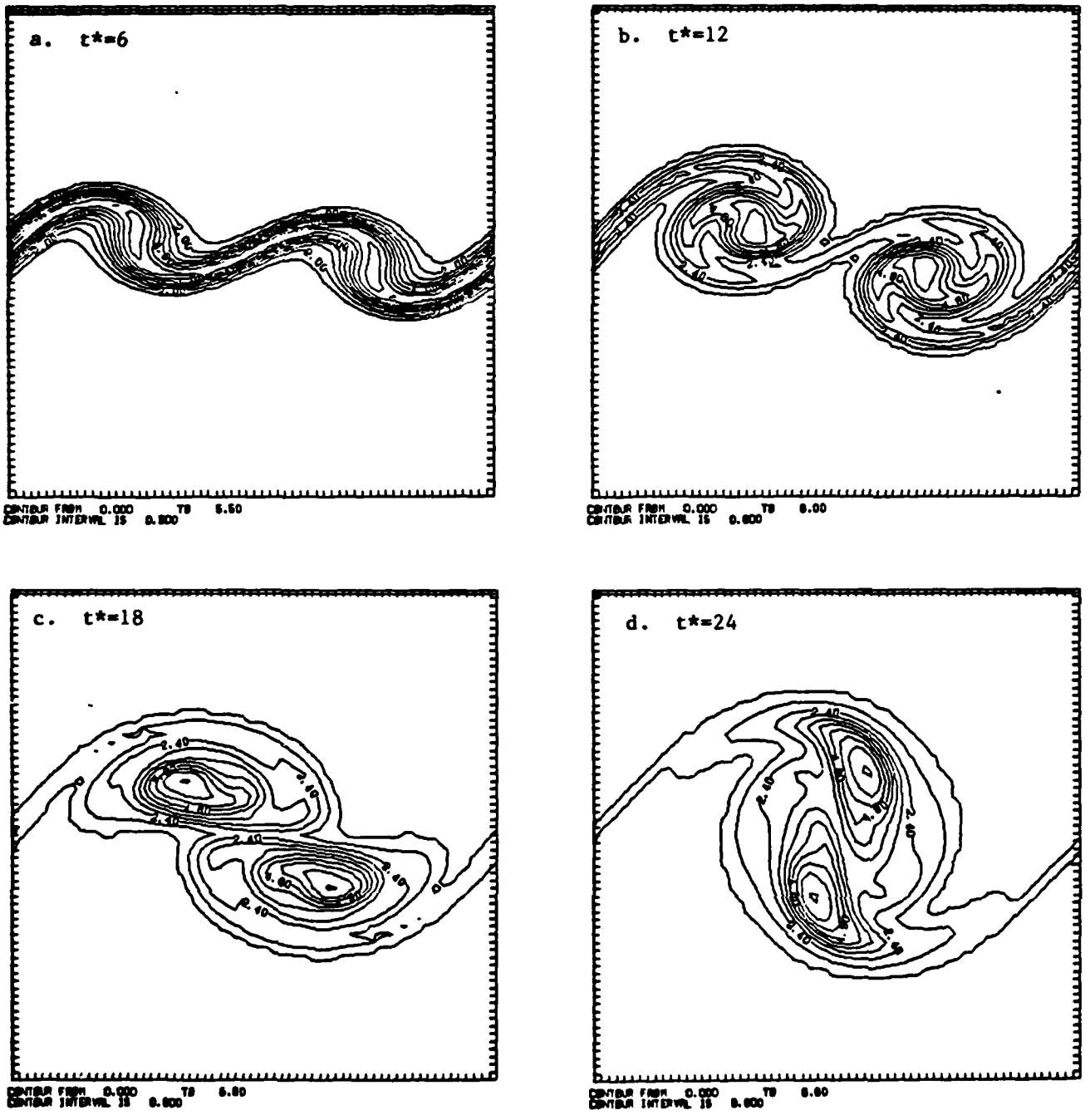

FIG 7. Plots of normalized temperature contours for a sequence of times (Case II).

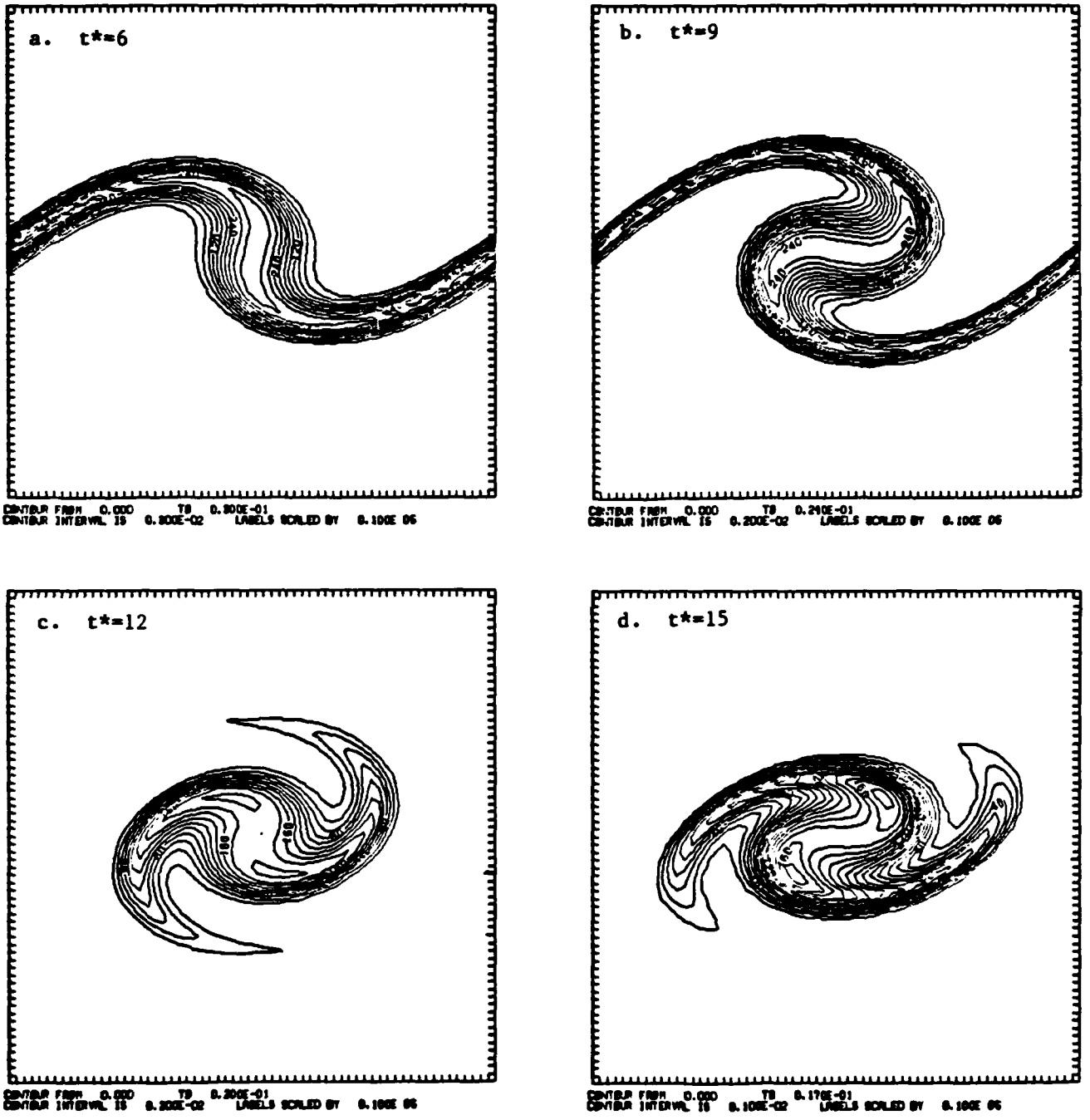

FIG 8. Plots of normalized reaction rate contours for a sequence of times (Case I).

APPENDIX B

Mixing and Chemical Reactions in a Spatially Developing Mixing Layer

MIXING AND CHEMICAL REACTIONS IN A SPATIALLY DEVELOPING MIXING LAYER

by

P. Givi and W.-H. Jou

Flow Research Company
21414-68th Avenue South
Kent, Washington 98032

February 1986

Manuscript Submitted for Presentation at
The Spring Technical Meeting of The Combustion Institute
Central States Section
Cleveland, Ohio, May 5-6, 1986

TP-152/02-86

MIXING AND CHEMICAL REACTIONS IN A SPATIALLY DEVELOPING MIXING LAYER

by

P. Givi and W.-H. Jou
Flow Research Company
Kent, WA 98032

ABSTRACT

Direct numerical simulations have been employed to study the effects of large coherent structures in a perturbed, time-dependent, spatially developing, reacting mixing layer. It is shown that the vortex dynamics has a significant influence on the enhancement of the chemical reactions, convolution of the reaction surface, and increase of product formation in the reaction zone of the layer. Furthermore, examination of some of the statistical quantities obtained from the results of direct numerical simulations indicates the asymmetric nature of the mechanism of mixing processes in the mixing zone of the layer.

1. INTRODUCTION

The advancement of supercomputer technology in recent years has had a major influence on increasing our understanding of the mechanisms of many complex physical phenomena such as turbulence. The availability of high-speed, large-memory computers has made it possible, in many cases, to simulate turbulent flow problems directly by solving the appropriate basic governing transport equations without any need for additional "turbulence modeling." Such modeling is required when these equations are statistically averaged. In a complex system such as a chemically reacting flow, modeling is extremely difficult because of our lack of knowledge on the detailed dynamics of the flow. Without using turbulence modeling, direct numerical simulations can provide the detailed information needed to increase our understanding of the physical processes involved in turbulent flows. An increase in understanding various aspects of the physics of turbulent reacting flows is evident in recent works (e.g., Riley et al., 1986).

Direct numerical simulations of turbulent reacting flows are presently applied to flows with limited dynamical and chemical parameter ranges. Continuing efforts in evaluating the advantages and also the limitations of this technique are required before the knowledge acquired can be applied to flows with practical parameter ranges. The application of direct numerical simulations to a flow with simplified geometrical configurations and well-controlled conditions is certainly the first step in understanding the physics and in evaluating the capabilities of the method.

A mixing layer, in which two parallel streams with different velocities begin to mix and react downstream of the trailing edge of a splitter plate partition, presents an ideal configuration for studying the physical processes in the mixing and reaction zones that exist in real diffusion-controlled combustors. Direct numerical simulations have been applied in studying a model problem of such flows with encouraging success (McMurtry et al., 1985; Riley et al., 1986). However, most of the previous work has employed a temporally developing mixing layer as a model. Temporally growing mixing layers refer to flows that, in a Galilean-transformed frame of reference, are assumed to evolve in time rather than in space. This is a good approximation for flows in which the difference between the freestream velocities of two streams is much less than the averaged velocity. This approximation allows simplifications in the formulation of periodic boundary conditions. A pseudospectral numerical method using Fourier series can then be employed to solve the appropriate transport equations.

Comparison of the simulation results obtained for a temporally developing mixing layer with experimental results is encouraging. The comparison shows that there is qualitative agreement between numerical simulations and laboratory data for the average reactant concentrations and the concentration correlations. However, there are some basic phenomena that cannot be explained by temporal simulations, such as (1) asymmetric mixing observed in mixing layer experiments (Koochesfahani, 1983), and (2) stablization, quenching, lift-off, and blowout of turbulent jet flames (Peters and Williams, 1983). A fundamental understanding of these phenomena requires detailed calculations of spatially growing flows. Here, we have developed a numerical technique that is capable of simulating a spatially developing mixing layer as a first step to further develop the technique of direct numerical simulations.

This paper presents some preliminary results of our two-dimensional flow simulations using the resulting code in an attempt to address the first of the above-mentioned phenomena associated with spatially growing flows. The flow fields under consideration are dominated by large-scale fluctuations associated with coherent structures. The chemical reaction that occurs between the reactants on two sides of the layer is assumed to be infinitely fast, so that complications due to complex kinetics need not be considered. Therefore, the transport of a conserved Shvab-Zeldovich scalar variable is computed. There is also a nonparallel growth mechanism of the layer mainly due to diffusion, vortex rollup, and subsequent pairing of the neighboring vortices. The effects of this nonparallel growth as well as the asymmetric mixing in the shear layer are studied. Analysis of flame extinction and lift-off phenomena requires consideration of nonequilibrium chemistry. This, as well as the effects of a three-dimensional random turbulence field, are presently under study and will be reported in the future.

In the next section, the governing equations, boundary conditions, and numerical algorithms for the present problem are discussed. Some sample results are presented in Section 3, and conclusions drawn based on these results are given in Section 4.

2. PROBLEM FORMULATION

The mixing layer under consideration is shown in Figure 1. The reactants are introduced as dilute traces in a carrier passive gas. The chemical heat release is assumed negligible. Therefore, the density of the mixture can be assumed constant and equal to that of the carrier gas. Under these assumptions, the hydrodynamics and the transport of chemical species are decoupled. The latter is governed by passive transport equations with a given hydrodynamic velocity field.

The velocity field satisfies the incompressible Navier-Stokes equations:

$$\rho\, L(\underline{U},\, \nu) = -\, \nabla P \tag{1}$$

$$\nabla \cdot \underline{U} = 0 \tag{2}$$

where P is the pressure, ρ is the density, which is assumed to be constant, ν is the kinematic viscosity, $\underline{U}$ is the velocity vector and L is the convective diffusive operator defined by

$$L(\underline{U},\, \nu) = \left(\frac{\partial \underline{U}}{\partial t}\right) + \underline{U} \cdot \nabla \underline{U} - \nu\, \nabla^2 \underline{U} \quad . \tag{3}$$

Species A is injected from the high-speed stream on the upper side of the plate, and species B is introduced from the low-speed stream. The chemical reaction between the species field is assumed to be fast and irreversible, such as

$$A + B \rightarrow C + D \quad . \tag{4}$$

The molar concentrations of the reactants (species A and B) and the product (say, species C) satisfy the following reaction-convection-diffusion equations:

$$L(C_A, D) = L(C_B, D) = - W \tag{5}$$

$$L(C_C, D) = W \tag{6}$$

where W is the reaction rate, and the stoichiometric coefficient is assumed to be equal to 1. The molecular diffusivities, D, of the species are assumed to be equal, i.e., $D_{ij} = D_{ji} = D$. If we define a Shvab-Zeldovich variable by

$$f = C_A + C_C \quad , \tag{7}$$

then the transport equation for f satisfies

$$L(f, D) = 0 \quad . \tag{8}$$

As shown by Williams (1985) and Bilger (1980), assuming an infinitely fast chemical reaction between species A and B, one would be able to determine the instantaneous fields of all the species involved.

In order to solve the set of Equations (1) through (8), boundary and initial conditions are needed. For the cross-stream direction, we assume the flow to be periodic with free-slip boundary conditions. At the inflow, the initial conditions for the Shvab-Zeldovich variable, f, are given by the following functional form:

$$f(0, Y) = \frac{1}{Y_o \sqrt{\pi}} \int_{-\infty}^{Y_o} \exp\left(-\frac{\epsilon^2}{Y_o^2}\right) d\epsilon \quad . \tag{9}$$

The initial conditions for the mean streamwise velocity are given by a hyperbolic tangent velocity profile, and the mean cross-stream velocity component is set equal to zero:

$$\underline{U} = [U(Y), 0] \tag{10}$$

$$U(Y) = U_1 [\tanh (2Y/\lambda) + 2] \tag{11}$$

where U_1 is the slow stream velocity, and λ is the vorticity thickness defined by

$$\lambda = \Delta U/(dU/dY)_{max} \quad . \tag{12}$$

The term ΔU is the difference between the velocities in the two layers.

It is well-known that a shear layer subject to white noise will develop coherent structures with predominantly the most unstable mode of its instability waves, and the subsequent pairing is caused by the subharmonic disturbance of the predominant mode. Therefore, in order to initiate the vorticity rollup and pairing, a small perturbation, in the form of the most unstable mode and its subharmonics, calculated from linear stability theory (Michalke, 1965; Monkewitz and Huerre, 1982) is added to this mean profile. In terms of stream function, we have

$$\psi = \psi_{mean} + \epsilon_1 \psi_1 + \epsilon_2 \psi_2 \tag{13}$$

where ψ_{mean} is the stream function associated with the mean flow, ψ_1 is the stream function for the most unstable mode, ψ_2 is that of the first subharmonic of the most unstable mode, and ϵ_1 and ϵ_2 are the amplitudes of the imposed perturbations. The presence of the fundamental mode in the mixing layer produces a single vortex rollup, and when the subharmonic perturbation is superimposed, a second rollup in the form of the merging of two vortices occurs (Ho and Huerre, 1984). The vortex rollup and pairing have dominant effects on the chemical reactions and the rate of formation of the products.

The downstream boundary is an artificial computational boundary and not a natural flow boundary. The boundary conditions there are difficult to formulate in a rigorous sense. We have assumed a zero-gradient condition on the velocity and species fields. This is not an exact representation of the outflow behavior. However, if the flow velocity is outgoing at the downstream boundary, which is the case here, the vorticity and species transport equations are hyperbolic when the molecular diffusion is small. Therefore, the upstream influence may be weak. The effects of this outflow boundary condition on the solution are later assessed by comparing results of the simulations for the same flow with various lengths of the computational domain.

The periodicity of the flow in the Y direction enables us to employ a pseudospectral numerical method (Gottlieb and Orszag, 1977) in that direction.

In the streamwise direction, however, an overall second-order finite difference scheme (Leonard, 1970) is employed with applications of a quadratic upwind differencing for the convection term where the leading dispersive truncation error of the second-order central scheme is removed. This scheme is expected to be accurate for the fine grids employed in these calculations. We use the Adams-Bashforth (Roache, 1972) technique for time discretization, which is a second-order-accurate scheme.

The computational domain was selected to be a region bounded by $(0 < X < 32\lambda)$ and $(-8\lambda \leq Y \leq 8\lambda)$. There are 128 equally spaced finite difference grid points in the X direction and 64 Fourier modes in the Y direction. Since the details of the chemistry are neglected and a fast chemistry model has been employed, this computational domain seems to be accurate enough for our solution procedure. The incremental time step was selected to be small enough to ensure both accuracy and stability. The value of Δt^* ($\Delta t^* = \Delta t\ \Delta U/\lambda$) was selected to be 0.0125.

The flow is conveniently characterized by two nondimensional parameters: first, the Reynolds number, $Re = \Delta U\ \nu/\lambda$, based on the initial shear layer thickness, the mean velocity difference across the layer, and the kinematic viscosity; and second, the velocity ratio, $R = \Delta U/(U_1 + U_2)$. The Shvab-Zeldovich variable is characterized by the value of the Peclet number, $Pe = \Delta U\ D/\lambda$. For the calculations reported below, we have selected moderate values of the Reynolds and Peclet numbers to ensure accuracy of the numerical simulations. As discussed by Ho and Huerre (1984), the two-dimensional vortex dynamics of the flow is not very sensitive to the Reynolds number, and only the shape of the vortices depends on the value of the Reynolds number employed. Therefore, simulations even at moderate Reynolds numbers provide useful information about the effects of the dynamics of vorticity on chemical reactions.

3. PRESENTATION OF RESULTS

Effects of Coherent Structures

As discussed in the previous section, a small perturbation at the inflow is required to trigger the initial vortex rollup. The perturbation levels, ϵ_1 and ϵ_2, are both set equal to 0.05. The velocity shear parameter R is equal to 0.5, and the values of the Reynolds and Peclet numbers are set equal to 50.

We present normalized vorticity contour plots at $t^* = 31$ for the case in which the most unstable mode is the only perturbation applied at $X = 0$. Figure 2 indicates the formation of rolled-up vortices at equal wavelengths. These vortices diffuse along the mixing layer as indicated by the decay of the peak value of the vorticity downstream. The formation of the rolled-up vortices is also evident in the contour plot of the Shvab-Zeldovich variable presented in Figure 3. From these two figures, it is clear that the perturbation at the inlet causes the rollup of the vorticity near the inlet. As the fluid is convected downstream, additional vortices are created at equal wavelengths from each other. The same behavior was also observed in numerical and experimental studies of McInville et al. (1985) in their studies of the large coherent structures in a forced shear layer. As the vortices reach the outflow boundary, the zero-gradient condition seems to allow them to travel out of the computational domain. Employment of this weak condition at the outflow may cause some errors near the outflow boundary. Previous numerical experiments by Givi (1981), however, show that the regions of the error associated with this condition are concentrated at a small area near the outflow and do not substantially affect the inner region of the computational domain. To assess the validity of this assumption, some computations were performed in two computational domains. The transverse dimensions of these two are identical, while one of the cases has a streamwise domain half the size of the other. The grid spacing in the streamwise direction is maintained. Comparison of the results clearly showed that the boundary conditions imposed at the outflow boundary do not affect the solution in the interior of the computational domain. Therefore, it seems justified that a zero-gradient boundary condition at the outflow is adequate for our purposes.

The effects of adding the perturbation corresponding to the first subharmonic mode at $X = 0$ are shown in Figure 4. In this figure, we present the rollup and merging of the vortices at times of $t^* = 31$ and $t^* = 39$. The merging of the vortices caused by the subharmonic perturbation, as computed here, has been observed in experiments of Ho and Huerre (1984). These merged vortices, again, diffuse and smear as they move downstream, and no further merging is observed. The same behavior was also observed in the calculations of Davis and Moore (1985). The vortex merging associated with this subharmonic mode is also clear from the Shvab-Zeldovich variable contour plots shown in

Figure 5. Again, the errors associated with the outflow boundary are concentrated only near the outflow and do not seem to affect the interior of the computational domain.

Contour plots of the computed product concentrations of the chemical reaction are presented in Figures 6 and 7. In Figure 6, only the perturbation associated with the most unstable mode is added to the mean flow, and in Figure 7, the perturbations associated with the fundamental frequency and its first subharmonic are added together to the mean flow. The regions of high product concentrations are, as expected, near the flame sheet, where the value of the Shvab-Zeldovich variable is equal to its stoichiometric value ($f = 0.5$). The vortex rollup brings unreacted species together from both streams to the chemical reaction zone. This region is marked by a very steep gradient of the chemical product near the braids of the vortices but is more diffusive in the core of the vortex. The vortex rollup increases the interface between the two streams by stretching the reaction zone and, therefore, increasing the amount of products generated. A comparison of these two figures indicates that the vortex merging results in increased formation of product in the mixing layer.

In these computations, the increase of flame sheet surface due to rollup of vortices is about 97 percent in comparison with unforced and nondiffusive computations, resulting in a 48-percent increase in total integrated products formed in the mixing layer. Merging of the vortices increases the flame sheet surface area by 163 percent and the total amount of products by 69 percent in comparison with the unforced and nondiffusive case. Bearing in mind the low level of initial disturbance, this high level of response may one day be exploited in a practical device.

Comparison of Figures 6 and 2 and also Figures 7 and 4 shows the similarity between the profiles of the vorticity and the chemical product. Both are high near the reaction zone, gradually diffusing outward with very similar profiles. This is to be expected, since the chemical reaction is to occur where the two reactants meet near the interface, which is also a region of high velocity gradient. The same conclusions were also drawn from earlier work on spectral calculations of temporally growing mixing layers (Riley et al., 1986). However, the asymmetric nature of the mixing mechanism in the shear layer is well represented in the spatially developing calculations, which are discussed next.

Statistical Variables

The results of direct numerical simulations have been studied to examine the validity of some of the previously used turbulence models in which the large coherent structures have not been taken into account. In previous work (Givi et al., 1984, 1985), many different possibilities for the closure of the hydrochemical equations in parallel shear flows were discussed. Among the models considered, the one with the best overall performance was the combination of a modeled joint probability density function (pdf) for the scalar variables and the K-ε model of turbulence (Launder and Spalding, 1972) for the hydrodynamic closure. A formulation based on a transport equation for the pdf of scalar variables has the advantage that the effects of chemical reactions appear in a closed form. However, models are needed for the closure of the molecular mixing term and also the turbulent convection. Givi et al. (1985) employed a qualesence/dispersion model for the closure of the molecular mixing term and a gradient diffusion approximation for the closure of the turbulent flux of the pdf. The results were compared with experimental data of Masutani and Bowman (1984) in similar hydrochemical conditions.

As far as the first few moments are concerned, the results obtained from the pdf transport equation are in reasonable agreement with experimental data. However, a major difference between the calculated and measured shapes of the probability density function is observed. This is indicated in Figure 8. In this figure, the pdf's of a nonreacting scalar variable (similar to the variable f defined above), are presented at a streamwise location. The profile obtained from experimental measurements of Masutani and Bowman (1984) is also presented on the same figure. The experimental results indicate an intermediate peak at a fixed value of the normalized concentration between the two delta functions at 0 and 1. In the predicted pdf's two spikes also exist at the normalized concentrations of 0 and 1, indicating the concentrations at freestreams. The height of the pdf in the middle region is in reasonably correct order-of-magnitude agreement with the experimental data. However, the location of the predicted pdf peak, with respect to the normalized concentration, gradually shifts as the layer is traversed. This is a major difference between the predicted and measured pdf's, as the modeled pdf transport equation is unable to predict the bimodal pdf's observed experimentally. As suggested by Givi et al. (1985), Koochesfahani (1983), and Masutani (1985), this discrepancy is mainly due to the shortcomings associated with the gradient diffusion

modeling of the turbulent flux of the pdf. In highly intermittent flows such as mixing layers, the continuity of turbulent flow is interrupted by the presence of the nonturbulent surrounding flows. Therefore, a simple gradient diffusion model is not expected to account accurately for this discontinuity.

Direct comparison of the shape of the pdf calculated from direct numerical simulations with that of experimental measurements is not possible due to the different Reynolds numbers used. However, a great deal of understanding of the influence of the large-scale structures in the mixing mechanism of the shear layer can be gained by examining the computed concentration pdf. The profile of the pdf's calculated from the results of the direct numerical simulation at the streamwise location of $X = 24\lambda$ is presented in Figure 9. This location corresponds to the point where the first merging between the two neighboring vortices occurs. It is indicated in this figure that at any cross-stream location away from the freestreams, the pdf has approximately three peak values. The first peak is closer to the low-speed fluid concentration, the second peak is closer to the high-speed fluid concentration, and the third peak is in a mixed concentration between the other two but closer to the high-speed side. The value of the pdf of the mixed concentration is larger than the pdf corresponding to other concentrations; also, the pdf of the concentration closer to the high-speed fluid side has a larger peak than the pdf of the low-speed concentration. This trimodal nature of the pdf, and also the fact that the mixed fluid pdf has a concentration near the high-speed side concentration, indicates the asymmetry of entrainment due to large-scale structures in the mixing region of the shear layer and also indicates that more fluid from the high-speed stream than the low-speed side is drawn into the mixing core of the layer. Comparison of this figure with Figure 8 indicates that the pdf's obtained here have a structure closer to the experimental observations of Masutani and Bowman (1984) than the previous calculations employing a modeled joint pdf transport equation (Givi et al., 1985). However, the calculated predominant peak of the pdf at the mixed fluid concentration is less pronounced than that observed experimentally by Masutani and Bowman (1984). This is possibly due to the fact that, in the present two-dimensional calculations, only the isolated effects of the large coherent structures are examined, and the effects of three-dimensional random turbulent fluctuations are not presented. Nevertheless, the results obtained from direct numerical simulations indicate that the mixing mechanism in the core of the shear layer

is asymmetric, and the mixed fluid has a concentration closer to the high-speed fluid concentration. This agrees with the experimental observations of Masutani and Bowman (1984) and Koochesfahani (1983). Three-dimensional flow simulations with random turbulent fluctuations are currently under study and are expected to result in better agreement with experimental data.

The mean and rms values of the conserved scalar obtained from the integration of the pdf profiles, presented above, are shown in Figure 10. This figure shows that the mean value of the concentration has an apparent "plateau" in the middle region of the shear layer. This "plateau" is at a concentration where a predominant peak occurs in the pdf (Figure 9). Similar behavior has also been observed in experimental measurements (Koochesfahani, 1983) and indicates the influence of the large-scale structure on the mean value of the concentration. The resulting rms values of the normalized non-reacting concentrations across the layer, obtained from the direct numerical simulations, indicate that there are two apparent maximums in the rms profile. These two points correspond to the location where the gradient of the mean value is highest. The same behavior was also observed in the experimental results of Masutani (1985). Calculations using a gradient diffusion model for the pdf turbulent transport are unable to predict this detailed behavior, as the calculations of Givi et al. (1985) indicate. The predicted results of the mean concentration by Givi et al. (1985) form a fairly smooth bell-shaped profile with a much less clear double "hump" in the middle region. However, the pdf calculation does show that the location of the rms maximums coincides with the location of the highest mean value.

From the discussion given above, it is clear that the intermittency caused by the large coherent structures contributes greatly to various vital statistics of turbulent flows. The results of direct numerical simulations can illuminate the qualitative behavior of large-scale structures in intermittent flow, such as the spatially developing mixing layer considered here. Quantitative comparison with the experimental data, however, is not yet possible. A three-dimensional flow simulation may be required for meaningful quantitative comparison with experimental results.

4. CONCLUSIONS AND FUTURE WORK

Numerical simulations have been performed for the large-scale vortex dynamics in a forced spatially developing, reacting mixing layer. A combination of a pseudospectral and a second-order finite difference technique has been employed to study the effects of the rollup of the vortices and of their merging on the rate of formation of the reaction product. As an earlier simulation (Riley et al., 1986; McMurtry et al., 1985) using a temporally developing approximation indicates, the vortex rollup and merging cause the stretching of the interface between the reactants, and thereby increase the stream surface area on which the chemical reaction occurs. In addition, the present simulations of a realistic spatially developing, chemically reacting mixing layer exhibit the asymmetric properties of the entrainment, which have been observed in experimental results (Masutani and Bowman, 1984).

The results of direct numerical simulations reported here and recent experimental measurements indicate the importance of large coherent structures in the mixing region of the shear layer. This suggests the need for better turbulence models in order to predict accurately the mechanism of mixing and chemical reaction in intermittent flows such as mixing layers.

Much remains to be done in our continuing effort in numerical combustion simulations. Consideration of a temperature-dependent reaction rate with intermediate Damkohler numbers has just been successfully finished for a temporally growing mixing layer (Givi et al., 1986) and should be included with the spatially growing mixing layer studied in this paper. This simulation can address the questions regarding the quenching and extinction of diffusion flames. Next, three-dimensional calculations involving a shear layer with a random turbulence field will be studied. This is a step toward simulations of turbulent flow and will provide a better understanding of the physics of turbulent diffusion flames. The effects of chemical heat release, at a temperature-dependent reaction rate, on the flow field and product formation in a spatially developing mixing layer would also be very interesting and will be addressed in future papers. Finally, it would be interesting to examine the effects of the vortex merging further by looking at the influence of even higher subharmonics and also the effects of phase relations between the different modes on the chemical reactions and the flame convolution in a spatially evolving mixing layer.

ACKNOWLEDGEMENTS

The calculations reported here were performed under the support of the Air Force Office of Scientific Research, Contract No. F49620-85-C-00067DEF. The authors have also appreciated the support of NASA Lewis Research Center in providing computer time.

REFERENCES

Bilger, R. W. (1980) in Turbulent Reacting Flows, edited by P. A. Libby and F. A. Williams, Springer-Verlag, New York, pp. 65-113.

Davis, R. W., and Moore, E. F. (1985) Physics of Fluids, Vol. 28, No. 6, pp. 1626-1635.

Givi, P. (1981) Department of Mechanical Engineering, Report CFD/81/11, Carnegie-Mellon University, Pittsburgh, Pennsylvania.

Givi, P., Ramos, J. I., and Sirignano, W. A. (1984) Progress in Astronautics and Aeronautics, Vol. 95, AIAA, New York, pp. 384-418.

Givi, P., Ramos, J. I., and Sirignano, W. A. (1985) Journal of Non-Equilibrium Thermodynamics, Vol. 10, pp. 75-104.

Givi, P., Jou, W.-H., and Metcalfe, R. W. (1986) submitted for publication.

Gottlieb, D., and Orszag, S. A. (1977) Numerical Analysis of Spectral Methods: Theory and Applications, SIAM, Philadelphia, Pennsylvania.

Ho, C.-M., and Huerre, P. (1984) Annual Review of Fluid Mechanics, Vol. 16, pp. 365-424.

Koochesfahani, M. M. (1983) Ph.D. Thesis, California Institute of Technology, Pasadena, California.

Launder, B. E., and Spalding, D. B. (1972) Lectures in Mathematical Models of Turbulence, Academic Press, New York.

Leonard, B. P. (1979) Computer Methods in Applied Mechanics and Engineering, Vol. 19, pp. 59-98.

Masutani, S. M. (1985) Ph.D. Thesis, Stanford University, Department of Mechanical Engineering, Stanford, California.

Masutani, S. M., and Bowman, C. T. (1984) WSS/CI paper 84-44.

McInville, R. M., Gatski, T. B., and Hassan, H. A. (1985) AIAA Journal, Vol. 23, No. 8, pp. 1165-1171.

McMurtry, P. A., Jou, W.-H., Riley, J. J., and Metcalfe, R. W. (1985) AIAA paper 85-0143. Also to appear in AIAA Journal.

Michalke, A. (1965) Journal of Fluid Mechanics, Vol. 23, Part 3, pp. 521-544.

Monkewitz, P. A., and Huerre, P. (1982) Physics of Fluids, Vol. 25, No. 7, pp. 1137-1143.

Peters, N., and Williams, F. A. (1983) AIAA Journal, Vol. 21, pp. 423-429.

Riley, J. J., Metcalfe, R. W., and Orszag, S. A. (1986) Physics of Fluids, Vol. 29, No. 2, pp. 406-422.

Roache, P. J. (1972) Computational Fluid Mechanics, Hermosa Publishers, Albuquerque, New Mexico.

Williams, F. A. (1985) Combustion Theory, The Benjamin Cummings Publishing Company, Inc., Menlo Park, California.

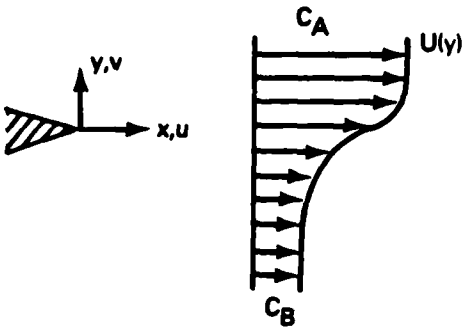

Figure 1. Problem Geometry.

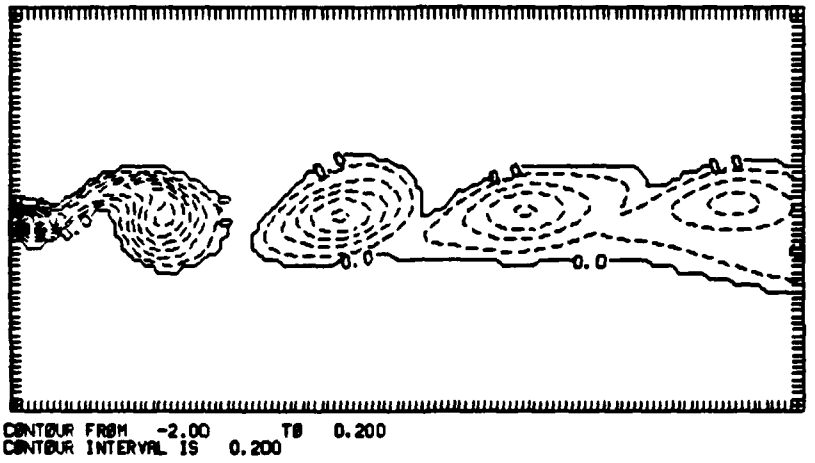

Figure 2. Plot of Vorticity Contour at $t^* = 31$. Single Rollup Case.

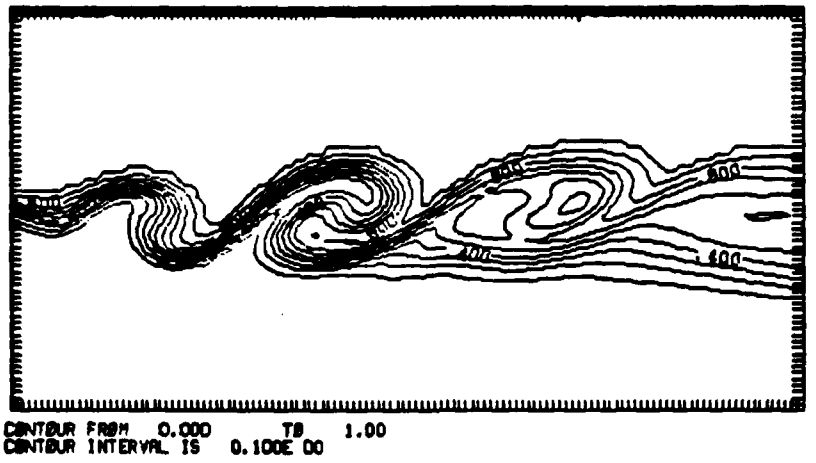

Figure 3. Plot of Shvab-Zeldovich Variable Contour at $t^* = 31$. Single Rollup Case.

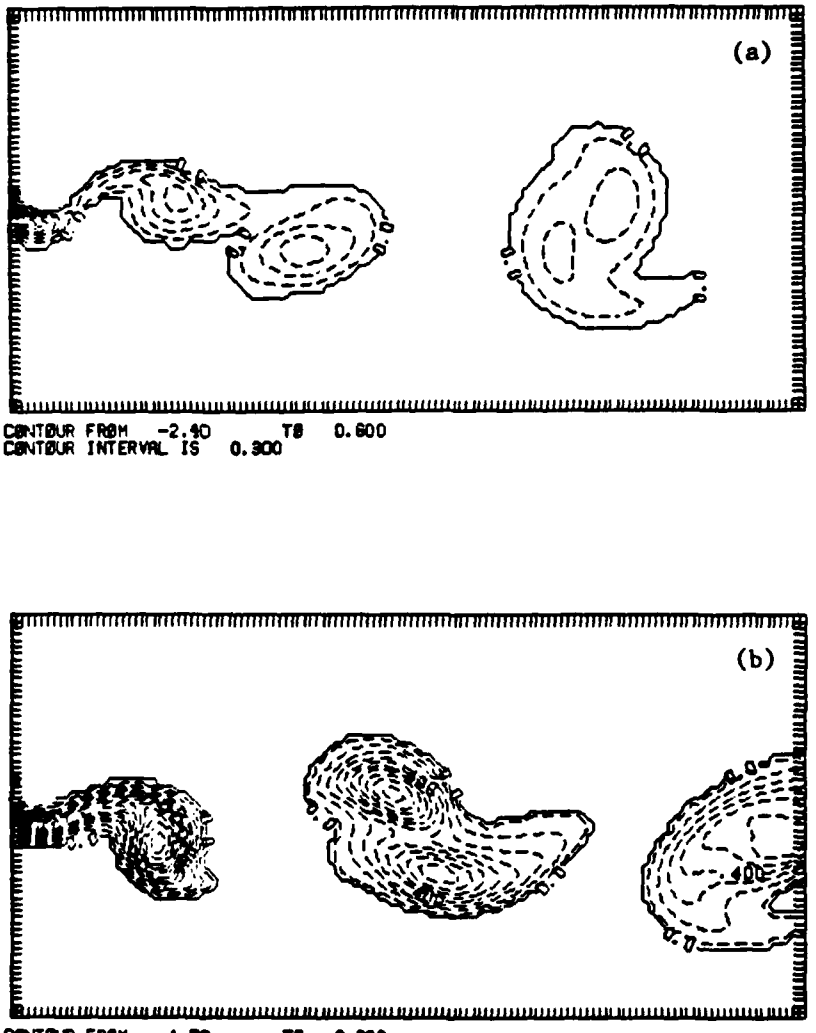

Figure 4. Plot of Vorticity Contour at (a) $t^* = 31$ and (b) $t^* = 39$. Double Rollup Case.

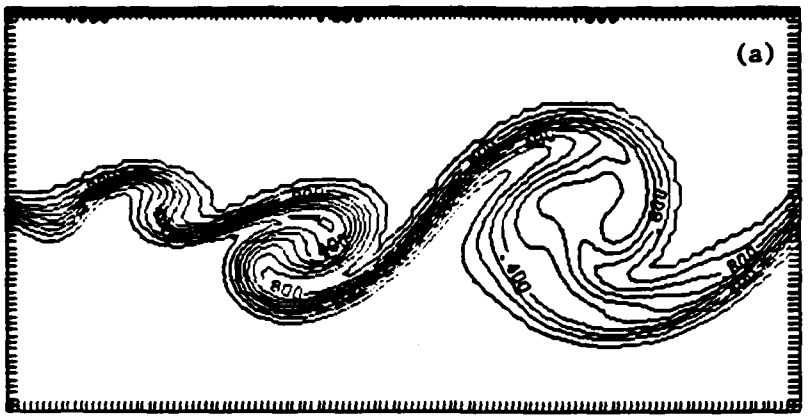

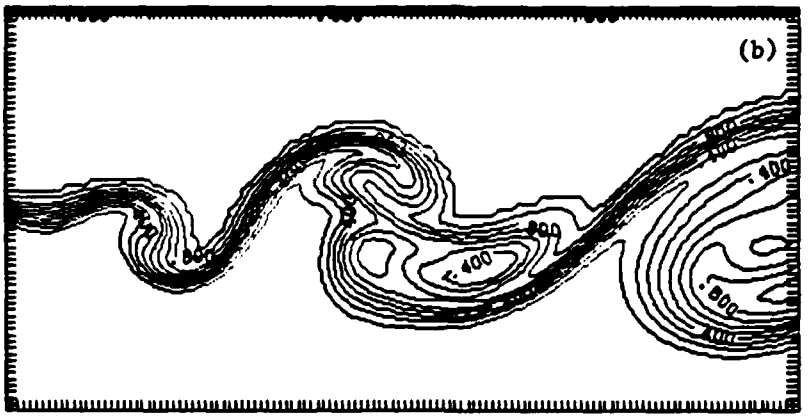

Figure 5. Plots of Shvab-Zeldovich Variable Contour at (a) $t^* = 31$ and (b) $t^* = 39$. Double Rollup Case.

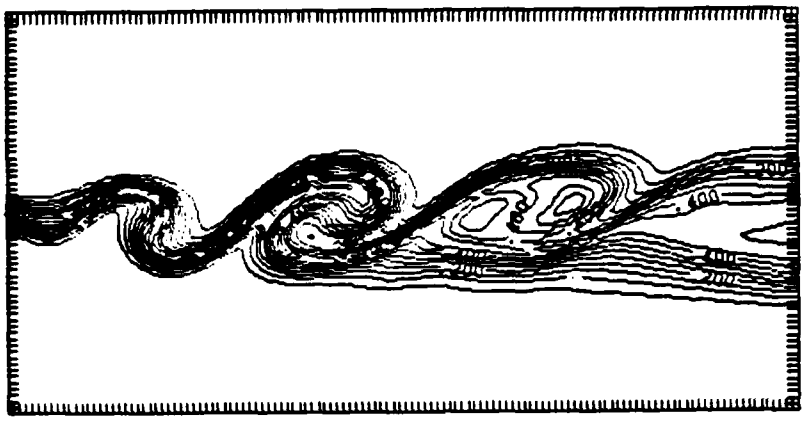

Figure 6. Plots of Product Concentration at $t^* = 31$. Single Rollup Case.

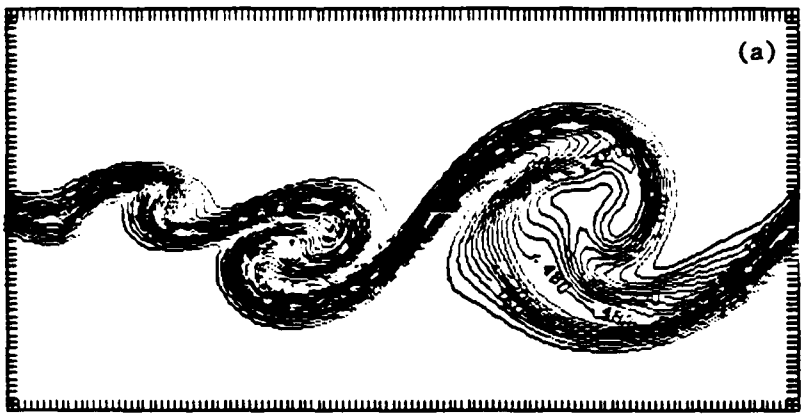

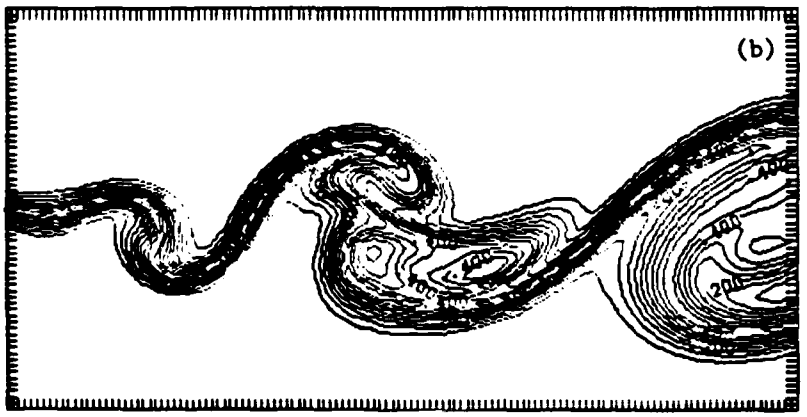

Figure 7. Plots of Product Concentration at (a) $t^* = 31$ and (b) $t^* = 39$. Double Rollup Case.

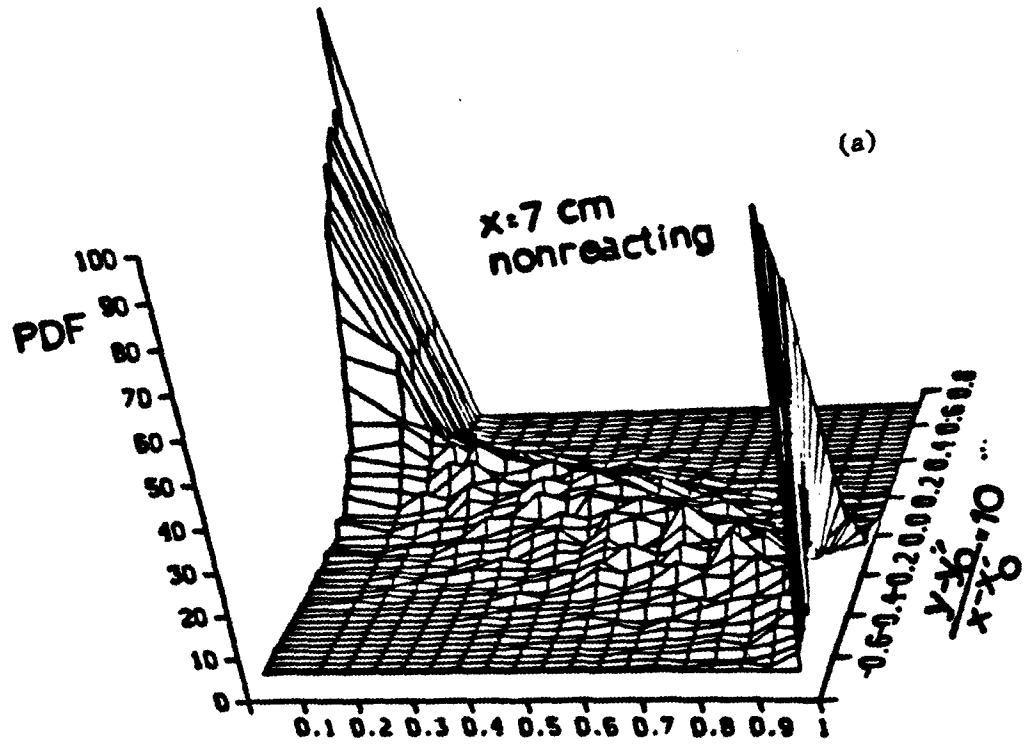

Figure 8. PDF of Shvab-Zeldovich Variable. (a) Givi et al. (1985); (b) Masutani and Bowman (1984).

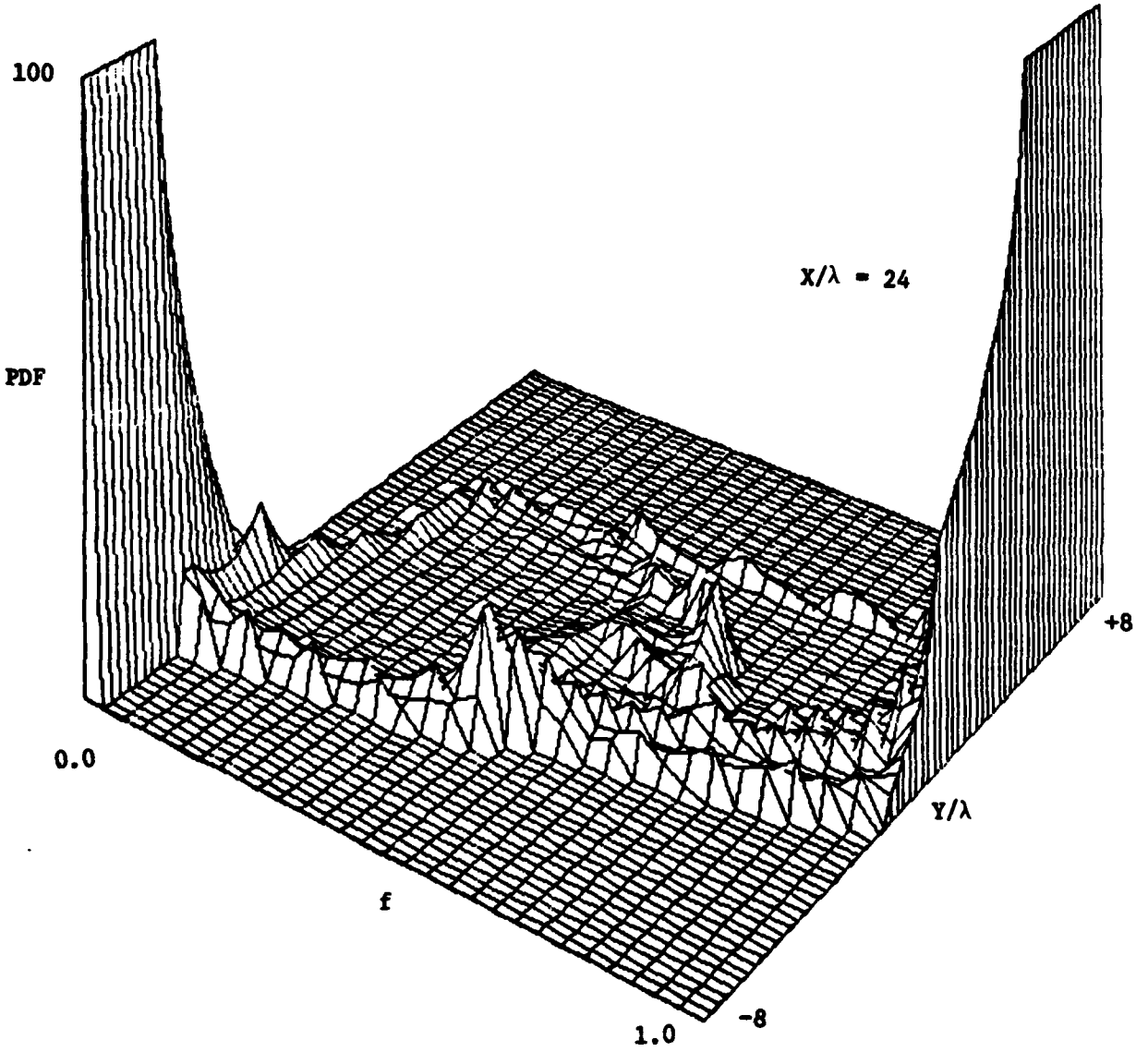

Figure 9. PDF of Shvab-Zeldovich Variable from Direct Numerical Simulations.

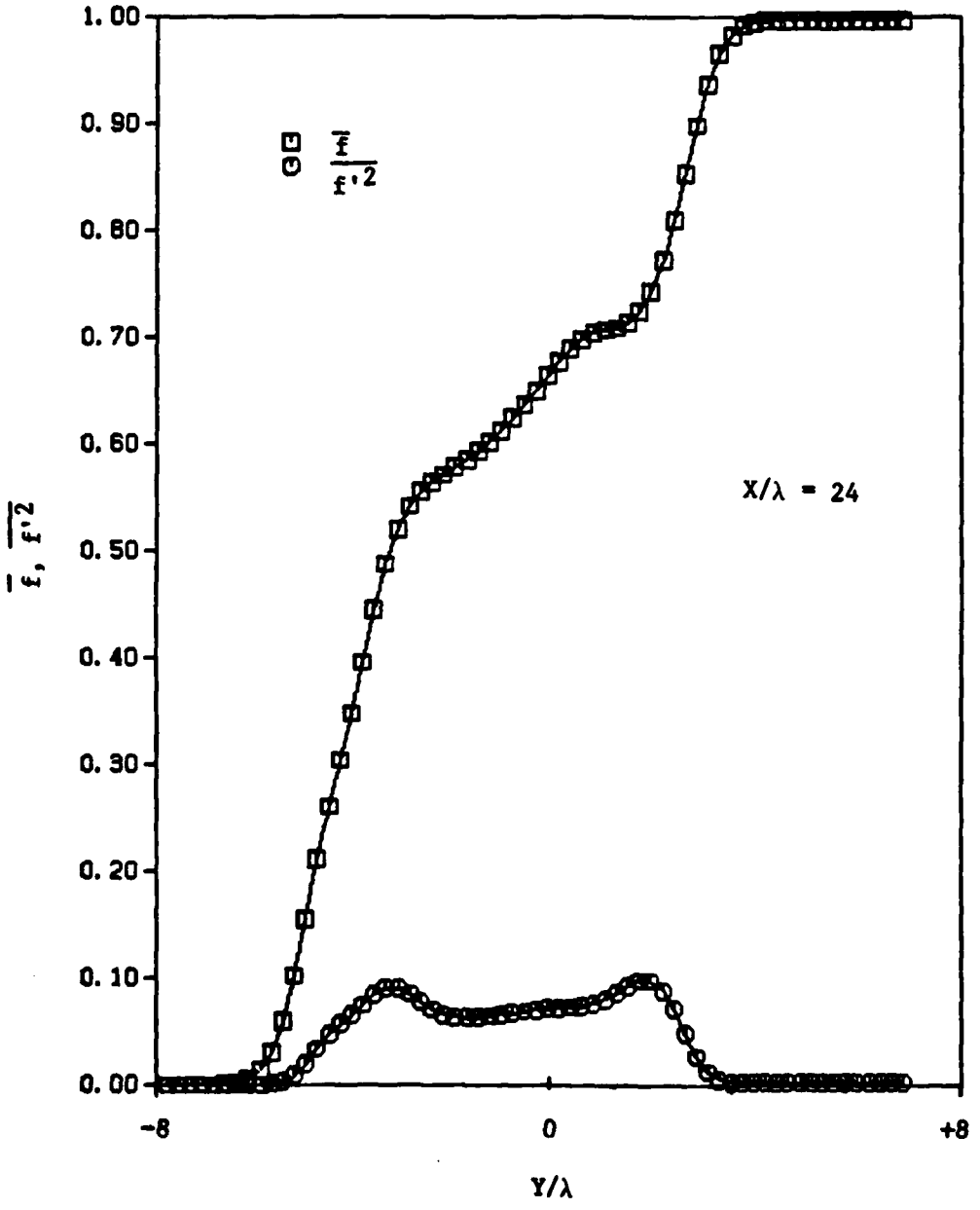

Figure 10. Profiles of Mean and RMS of Shvab-Zeldovich Variable.

END

12-86

DTIC